Talanta 269 (2024) 125519

Contents lists available at ScienceDirect

Talanta

journal homepage: www.elsevier.com/locate/talanta

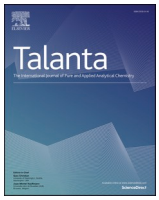

Unravelling the *in vitro* and *in vivo* potential of selenium nanoparticles in Alzheimer's disease: A bioanalytical review

David Vicente-Zurdo [a,b,*], Noelia Rosales-Conrado [a], María Eugenia León-González [a,*]

[a] *Dpto. Química Analítica, Facultad de Ciencias Químicas, Universidad Complutense de Madrid, 28040, Madrid, Spain*
[b] *Centre for Metabolomics and Bioanalysis (CEMBIO), Department of Chemistry and Biochemistry, Facultad de Farmacia, Universidad San Pablo-CEU, CEU Universities, Urbanización Montepríncipe, 28660, Boadilla del Monte, Madrid, Spain*

A R T I C L E I N F O

Handling Editor: Prof. J.-M. Kauffmann

Keywords:
Selenium nanoparticles
Alzheimer's disease
Bioanalytical methods
Beta-amyloid protein
In vitro cell evaluation
In vivo studies

A B S T R A C T

Alzheimer's disease (AD) is a devastating neurodegenerative disorder characterized by progressive cognitive decline and the accumulation of beta-amyloid plaques and tau tangles in the brain. Current therapies have limited efficacy, prompting the search for novel treatments. Selenium nanoparticles (SeNPs) have emerged as promising candidates for AD therapy due to their unique physicochemical properties and potential therapeutic effects. This review provides an overview of SeNPs and their potential application in AD treatment, as well as the main bioanalytical techniques applied in this field. SeNPs possess antioxidant and anti-inflammatory properties, making them potential candidates to combat the oxidative stress and neuroinflammation associated with AD. Moreover, SeNPs have shown the ability to cross the blood-brain barrier (BBB), allowing them to target brain regions affected by AD pathology. Various methods for synthesizing SeNPs are explored, including chemical, physical and biological synthesis approaches. Based on the employment of algae, yeast, fungi, and plants, green methods offer a promising and biocompatible alternative for SeNPs production. *In vitro* studies have demonstrated the potential of SeNPs in reducing beta-amyloid aggregation and inhibiting tau hyperphosphorylation, providing evidence of their neuroprotective effects on neuronal cells. *In vivo* studies using transgenic mouse models and AD-induced symptoms have shown promising results, with SeNPs treatment leading to cognitive improvements and reduced amyloid plaque burden in the hippocampus. Looking ahead, future trends in SeNPs research involve developing innovative brain delivery strategies to enhance their therapeutic potential, exploring alternative animal models to complement traditional mouse studies, and investigating multi-targeted SeNPs formulations to address multiple aspects of AD pathology. Overall, SeNPs represent a promising avenue for AD treatment, and further research in this field may pave the way for effective and much-needed therapeutic interventions for individuals affected by this debilitating disease.

1. Introduction

Neurodegenerative diseases are characterized by progressive impairment in various cognitive aspects, such as memory, language, executive capacity, spatial vision, personality and behavior [1]. Dementia is the first leading cause of disability and the second leading cause of death worldwide [2]. They currently affect to more than 50 million people worldwide, and projected to reach 152 million by 2050, being ageing the main risk factor [3–5]. However, approximately 75 % of people with dementia are not officially diagnosed [6]. Currently, there are no effective treatments for these neurological disorders, leading to significant socio-economic costs [5].

The four most prevalent neurodegenerative diseases are Alzheimer's disease (AD), Parkinson's disease, amyotrophic lateral sclerosis and Huntington's disease [7–9]. Among them, AD is the most widespread, affecting one in ten people over the age of 65, and accounting for 60–80 % of all dementia cases [5]. AD often coexists with other neurodegenerative diseases, which is called "mixed dementia" [3]. It is characterized by progressive memory impairment and increasing cognitive dysfunction, due to massive loss of cortical and hippocampal neurons. AD is histologically manifested by extracellular deposition of beta-amyloid (Aβ) protein plaques, intracellular formation of neurofibrillary tangles (NFTs) of hyperphosphorylated tau protein (p-tau) and neuroinflammation [3,10]. Symptoms usually start at the age of 60,

* Corresponding authors.
E-mail addresses: davidvic@ucm.es, david.vicentezurdo@ceu.es (D. Vicente-Zurdo), leongon@ucm.es (M.E. León-González).

https://doi.org/10.1016/j.talanta.2023.125519
Received 25 July 2023; Received in revised form 30 November 2023; Accepted 3 December 2023
Available online 7 December 2023

observing apathy, depression and difficulty remembering conversations, names or recent events in early stages of the disease [11]. In later stages, communication disorders, personality changes, confusion and disorientation become common. Finally, the patient has great difficulty in speaking, swallowing and even walking [12]. More than 50 % of deaths derived from AD are failures of respiratory system, while circulatory system accounts for 25 % [13].

Although AD origin remains unclear, several hypotheses have tried to explain it. The first one to be considered was the "*cholinergic hypothesis*", proposed in 1976 [14]. This hypothesis considered certain alterations that interfere with the normal functioning of cholinergic neurons, such as choline acquisition, impaired acetylcholine (ACh) and butyrylcholine (BCh) release and deficits in axonal transport [15,16]. Through post-mortem studies of brains of AD patients, there is evidence that the activity of the enzyme choline acetyltransferase, responsible for the synthesis of the neurotransmitter ACh, is lower in the amygdala, hippocampus and cortex. For this reason, ACh is in lower concentration in the synapses of AD patients, presenting a failure of the cholinergic system [17]. To address this deficit of ACh and BCh, some of the current strategies are based on the inhibition of acetylcholinesterase (AChE) and butyrylcholinesterase enzymes. By using acetylcholinesterase and butyrylcholinesterase inhibitors, the degradation of ACh and BCh is prevented, and the integrity of the cholinergic system is preserved as much as possible [18]. However, the effect of these inhibitors is limited and, although they improve the quality of life of people diagnosed with AD, they fail in slowing down the progression of the disease.

The "*amyloid cascade hypothesis*", proposed in 1991, is the most widely agreed explanation of how AD is triggered [19,20]. In this hypothesis, the aggregation of Aβ protein is responsible for neuronal damage and death, which leads to the development of AD. Here, AD begins with an imbalance between the generation and clearance of $A\beta_{42}$ protein due to erroneous proteolysis of amyloid precursor protein (APP), resulting in its accumulation on the outside of neurons and neurites, forming extracellular amyloid plaques. This leads to a loss of interneuronal communications, affecting synapses [21]. Furthermore, $A\beta_{42}$ aggregation reduces mitochondrial respiration in neurons and astrocytes [22].

Tau protein, present in high concentrations in neurons, contributes to the stabilization of microtubules [23]. However, the primary event of $A\beta_{42}$ aggregation leads to the formation of NFTs of p-tau inside neurons. The intracellular accumulation of NTFs prevents the passage of essential nutrients and molecules into the cells, hindering their normal functioning and triggering neuronal death [24].

In addition, neuroinflammation has also been shown to play a key role in the development of AD. In AD patients, there is up to a 5-fold increased concentration of microglia around amyloid plaques and neurons with intracellular NFTs. The $A\beta_{42}$ protein binds to and destroys these glial cells, releasing factors that induce inflammation, triggering an immune response and increasing tau hyperphosphorylation [25]. Another factor favoring the development of AD is the oxidative stress produced inside the brain [22,26]. Together, these events lead to the inevitable neurodegeneration and clinical diagnosis of AD [27,28].

On the other hand, metals are present in the environment mainly due to anthropogenic activities. As a result, humans are chronically exposed to essential metals (biometals) such as iron, copper or zinc, and toxic metals such as mercury, cadmium or aluminum, disrupting homeostasis in the body [29]. Essential metals, or biometals, such as iron, copper and zinc, have an optimal concentration at which they are beneficial to the humans. However, if they are either deficient or in excess, they can cause health problems [29]. In contrast, for toxic metals such as mercury, cadmium or aluminum, their toxic effects are observed at exceptionally low concentration levels ($\mu g\ kg^{-1}$) [29].

The hypothesis that best explains the aggregation of $A\beta_{42}$ fibrils to form senile plaques is the so-called "*metal ion hypothesis*". According to this hypothesis, the dyshomeostasis in the concentrations of essential biometals such as Fe, Cu and Zn favors $A\beta_{42}$ protein aggregation, triggering the events described in the "*amyloid cascade hypothesis*", with these hypotheses entering into an inevitable synergy [20,30].

Several biometals function as cofactors for enzymatic activity, mitochondrial function and neuronal function within the central nervous system (CNS), and alterations in the homeostasis of these biometals may lead to the development of certain diseases [31]. Through post-mortem studies of brains from patients diagnosed with AD, it has been observed that senile plaques composed mainly of amyloid fibrils also contain metals such as iron, copper and zinc that have collaborated in their aggregation [26]. In healthy patients, biometals remain up-regulated and in low concentrations. However, copper concentrations in brains of AD patients are 5.7 times higher than in healthy brains, as are iron and zinc, 2.8 and 3.1 times respectively [32].

Selenium (Se), a trace element with notable physiological and pharmacological properties, plays a vital role in cellular function, detoxification, redox homeostasis, and immune protection. The trace element selenium and its redox cycles involving forms such as selenium (II), sodium selenate (VI), and sodium selenite (IV) exhibit efficient inhibition of reactive oxygen species (ROS). In drug delivery and nanomedicine, selenium's potential has attracted considerable attention. Nano-sized elemental selenium (Se°) offers advantages over other forms, but effective gastrointestinal absorption requires this nano-size [33].

Research has extensively focused on Se's protective effects against neurodegenerative diseases, especially AD. Se inhibits Aβ fibril formation, breaks down existing fibrils, and exhibits antioxidant activity, crucial in AD [34]. However, conventional Se supplements have limited absorption and considerable toxicity, necessitating innovative carrier systems to enhance bioavailability and enable controlled release [35].

The intake of moderate amounts of organic selenium provides multiple benefits to the organism. The consumption of selenium-enriched yeast improves spatial memory and learning, increases neuronal activity, supports synaptic preservation, and reduces tau levels and its hyperphosphorylation, making it a promising candidate against the progression of AD [36]. Selenium provides benefits against other types of diseases, such as cancer and thyroid [37]. Its antioxidant properties come largely from its presence in various enzymes, such as glutathione peroxidases (GPx) [38]. Selenium also has a high facility for chelating biometals whose oxidative stress favors the development of AD, such as Cu and Fe, and biometals involved in matrix metalloproteases (MMPs), such as Zn [39]. In addition, it is able to chelate toxic metals, such as Hg, Cd and Al, and to reduce their toxicity through the formation of inert complexes [40–42].

However, selenium properties depend on the chemical form in which it is present, differing in oxidation state, isotopic composition or chemical structure [43]. This structure can vary depending on the ligands attached or whether the selenium is nanoparticulated [44]. Selenium nanoparticles (SeNPs) possess varied physicochemical properties, as they can be chemo preventive, anticarcinogenic and antimicrobial [45]. Their role in the treatment of AD is promising, being able to penetrate the blood-brain barrier (BBB) given their size [46]. The range of selenium from essential to toxic is very narrow, which makes SeNPs with low toxicity ideal candidates for treating diseases such as arthritis, diabetes and cancer [47].

The surface of SeNPs, once synthesized by chemical and/or biogenic processes, can be functionalized with a plethora of ligands that stabilize them and provide additional characteristics. This wide range of beneficial properties that can be brought to SeNPs constitutes a new avenue for the synergistic treatment of a multitude of diseases [48]. In addition, SeNPs can be coated with a multitude of compounds with the aim of reducing their toxicity and even reducing Aβ aggregation. This inhibition of Aβ fibril formation can be accomplished by SeNPs disrupting hydrophobic and electrostatic interactions in amyloid nucleation [49].

The typical timeline for the development of SeNPs as pharmaceutical agents for AD encompasses several key stages. Initial stages involve the synthesis and characterization of SeNPs using diverse methods,

including chemical, physical, and biological approaches. A focus on understanding their physicochemical properties is essential for subsequent therapeutic applications. Following synthesis, emphasis is placed on *in vitro* studies to assess SeNPs' interactions with molecular targets associated with AD pathology. This phase identifies specific mechanisms through which SeNPs can intervene in the disease process. Subsequent stages concentrate on optimizing SeNP formulations, considering factors such as size, surface modifications, and drug loading capabilities. This aims to enhance bioavailability and facilitate targeted delivery to the brain. Transitioning to *in vivo* studies involves assessing the efficacy and safety of SeNPs in animal models, particularly in the context of AD. It is essential to explore SeNPs' ability to traverse the BBB and their impact on cognitive functions. Current efforts focus on clinically translating SeNPs, investigating safety profiles, pharmacokinetics, and therapeutic potential in human subjects. Clinical trials are underway to evaluate the effectiveness of SeNPs as a targeted intervention for AD. Ongoing and future directions include addressing challenges such as scale-up for mass production, refining delivery methods, and further elucidating nuanced molecular interactions. Additionally, efforts are directed towards developing innovative strategies to enhance overall therapeutic efficacy of SeNPs in the treatment of AD. This comprehensive overview underscores the multidimensional journey of SeNPs, highlighting their evolution from synthesis to potential pharmaceuticals for AD treatment.

While the literature contains some review articles on SeNPs, including their synthesis, characterization and biomedical applications [50,51], the novelty of this study lies in the comprehensive integration of various selenium nanoparticles, encompassing their characterization and *in vitro/in vivo* simultaneous evaluation. This review is specifically oriented towards the exhaustive assessment of their neuroprotective effects against AD. Simultaneously employing *in vitro* and *in vivo* studies contributes to a comprehensive and up-to-date understanding, providing a holistic perspective on this field. Therefore, in the present review, a literature compilation on the different synthesis processes of SeNPs, including their various stabilizers, as well as their *in vitro* and *in vivo* studies will be carried out to further investigate their potential role against AD. At the end, future perspectives for their use as anti-AD drugs will be discussed.

2. Selenium nanoparticles and synthesis methods

2.1. Selenium and nano selenium

SeNPs have surfaced as unique selenium species, exhibiting remarkable prophylactic and therapeutic properties, offering dual synergistic effects by delivering therapeutic cargo and enhancing anticancer activity. Recent studies have further expanded the scope of nano-sized selenium, exploring its potential for diverse biological activities, including serving as antibacterial and antifungal agents [52] (Fig. 1).

SeNPs have gained global recognition for their remarkable health benefits, leading to their widespread application in therapeutic settings. Compared to inorganic selenium, SeNPs exhibit lower toxicity, higher efficiency in combating free radical species, and favorable bioavailability. Additionally, SeNPs demonstrate lower toxicity when compared to other organic and inorganic compounds like selenate, selenite, and selenomethionine [35].

SeNPs play vital roles in numerous physiological and metabolic processes, including immune system regulation and antioxidant defense. Their remarkable ability to penetrate biological cells and tissues suggests potential efficacy in combating oxidative stress and inflammation. As a result of these distinct advantages, SeNPs have captivated significant interest from scientists for their potential use in treating neurological diseases. Recent studies have focused on the relationship between altered microbiota and neurological disorders, highlighting the significant impact of the synergetic communication between the CNS and gut on the development of AD [53].

In a study carried out by Lei Qiao et al., it was demonstrated that the administration of SeNPs enriched with *Lactobacillus casei* ATCC 393 effectively prevented cognitive dysfunction in mice with Alzheimer's disease. This positive outcome was attributed to the modulation of the microbiota-gut-brain axis. The results indicated that *L. casei* ATCC 393-SeNPs hold great promise as a safe and beneficial selenium nutritional supplement, potentially serving as a food additive to help prevent neurodegenerative diseases [54].

Since oxidative stress is a key factor in the development of neurodegenerative diseases, there is a growing emphasis on creating nanoparticles (NPs) with enhanced antioxidant capabilities. Numerous studies have highlighted the potential of SeNPs in Alzheimer's disease,

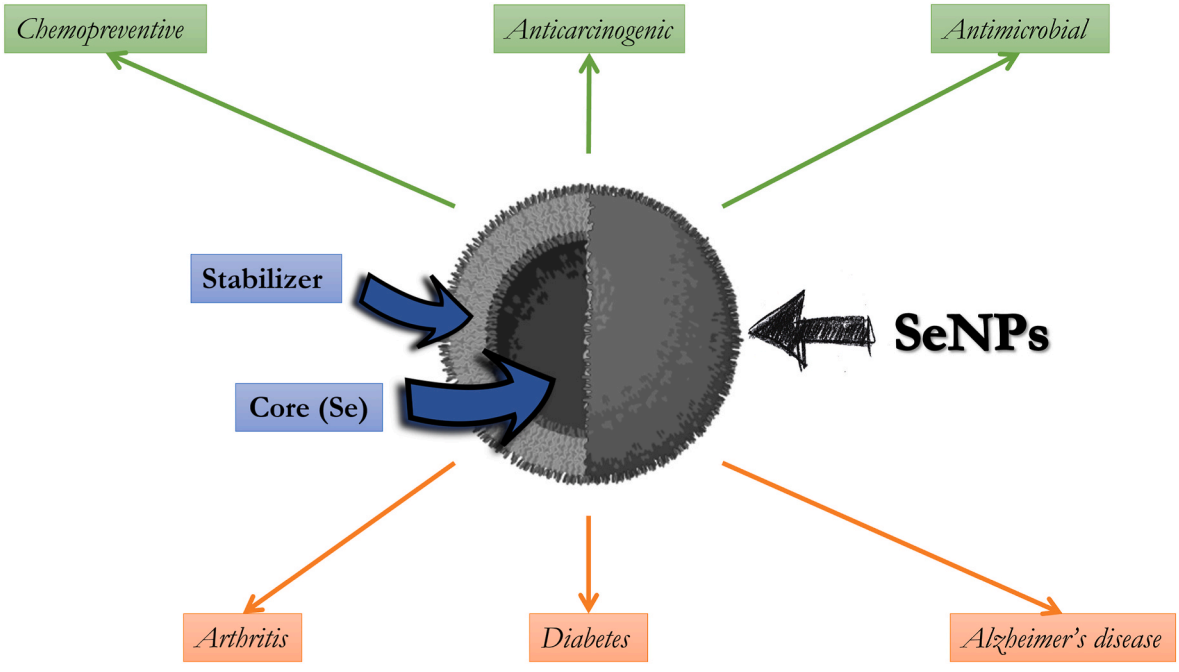

Fig. 1. SeNPs general structure, bioactive properties and possible therapeutic targets.

showcasing their ability to hinder the aggregation of amyloid-Aβ protein and their capability to traverse the BBB [53].

Yang et al., conducted a study where they synergistically combined the distinctive Aβ absorption characteristic of SeNPs with the natural antioxidant resveratrol (Res) to create Res@SeNPs. This combination demonstrated a remarkable synergistic effect against Cu^{2+}-induced $A\beta_{42}$ aggregation and ROS generation, effectively safeguarding PC12 cells from cell death induced by $A\beta^{42}$-Cu^{2+} complexes [55].

Abozaid et al., developed Res-SeNPs and investigated their impact on neurochemical and histopathological aspects in a rat model of Alzheimer's disease, induced by $AlCl_3$ at a dose of 100 mg kg^{-1} day^{-1} for 60 days. The Res-SeNPs exhibited a beneficial effect on cholinergic deficits and led to the clearance of amyloid-Aβ, showcasing their potential in alleviating AD-related impairments. Beyond their antioxidant properties, the formulated Res-SeNPs also demonstrated anti-inflammatory effects, contributing to improved neurocognitive function and modulation of signaling pathways associated with AD therapy [56].

Li et al., devised a novel nanocomposite comprising small Res selenium-peptide, which facilitated the use of Res in combating neurotoxicity induced by Aβ aggregates and alleviating gut microbiota disorder in AD model mice induced by $AlCl_3$ and D-galactose. This groundbreaking approach presents a promising new strategy for treating AD [57].

Moreover, Yang et al., formulated Res-loaded selenium nanoparticles/chitosan nanoparticles (Res@SeNPs@Res–CS–NPs) to modulate gut microbiota in cases of AD with metabolic disorders. The treatment with Res@SeNPs@Res–CS–NPs effectively regulated the levels of gut microbiota linked to oxidative stress, inflammation, and lipid deposition. Furthermore, it substantially improved cognitive function in AD mice with metabolic disorders, emphasizing its potential in preventing cognitive impairments associated with AD [58].

Sialic acid-modified SeNPs also demonstrated impressive capabilities in inhibiting the Aβ aggregation process and exhibited the ability to cross the BBB effectively [59]. While Gao et al., developed selenium-chondroitin sulphate (CS) nanoparticles (CS@SeNPs) and examined their therapeutic impact on *in vitro* AD models. CS@SeNPs demonstrated a remarkable ability to inhibit amyloid-Aβ aggregation and provided protection to SH-SY5Y cells against $A\beta_{1\text{-}42}$-induced cytotoxicity. Moreover, CS@SeNPs showed potential in suppressing Aβ aggregation, minimizing cytoskeletal damage, mitigating oxidative stress, and attenuating tau protein hyperphosphorylation. This multifunctional capacity makes CS@SeNPs a potential candidate for the treatment of AD [34].

Additionally, Ji et al., conducted a study to assess the impact of CS@SeNPs on mice with AD, resulting in the alleviation of anxiety and significant improvement in spatial learning and memory impairment [60].

In their research, Gholamigeravand et al., explored the potential of a combination therapy involving SeNPs and stem cells to mitigate neurotoxicity in an animal model of AD. The synergistic effect of this combined therapy proved to be more effective in reducing the deposition of Aβ and elevating the concentration of brain-derived neurotrophic factor (BDNF) [61].

2.2. Physical characteristics of SeNPs

Nanomaterials possess distinctive physicochemical properties, including small size, a substantial surface area, and high reactivity. Studies have highlighted that when appropriately modified, NPs can serve as valuable tools for drug delivery, imaging, and therapeutic interventions in AD. NPs generally exhibit a large surface area, allowing for significant adsorption capabilities. Specifically, certain NPs can bind with Aβ, effectively slowing down the fibrillation processes of Aβ [62].

The size of nanomaterials plays a crucial role in overcoming both extracellular and intracellular barriers for effective nanoparticle-mediated delivery. Cellular processing of NPs is greatly influenced by their size, which governs the extent and mechanism of retention and clearance in the body. The biological activities of NPs are also influenced by their size, with smaller NPs being more active than larger ones. Notably, NPs smaller than 10 nm are rapidly eliminated through the kidneys, while those in the size range of 10–150 nm are sequestered in the bone marrow. Particles larger than 200 nm undergo splenic clearance, whereas NPs in the range of 50–500 nm are retained in the body for longer periods and are slowly cleared through the liver. Finally, particles larger than 500 nm are removed from the body by macrophages and monocytes of the reticuloendothelial system.

SeNPs represent a cutting-edge source of selenium, offering optimal bioavailability *in vivo* while minimizing the risk of selenium toxicity. Studies indicate that SeNPs exhibit superior biocompatibility and degradability compared to noble metals like silver, gold, and platinum. Furthermore, when compared to organic and inorganic selenium forms, various nano-sized selenium formulations have displayed lower toxicity alongside enhanced antioxidant and anti-tumor activities. Notably, chemogenically synthesized SeNPs demonstrated toxicity levels seven times lower than sodium selenite in mice and exhibited a higher LD_{50} than selenomethionine. Consequently, nanoforms of selenium have proven to possess significant advantages over micro or macroforms, making them highly promising for a range of biomedical and dietary supplement applications [52].

Understanding the physical characteristics of NPs essential because their shape and size profoundly impact their interactions with cells and tissues. For instance, Se nanowires exhibit higher photoconductivity, whereas spherical-shaped SeNPs have demonstrated superior biological activities. The antioxidant properties of NPs are also size-dependent. SeNPs have shown the ability to scavenge free radicals in a manner dictated by their size (ranging from 5 to 200 nm). Additionally, the functionalization of NPs with other substances relies on the shape and size of the NPs. For example, the effectiveness of chitosan as an antioxidant and antitumor agent is intricately linked to the characteristics of SeNPs.

The method of synthesis significantly impacts the shape and size of NPs, consequently influencing their medicinal properties. Various forms of SeNPs exist, including rod-like, hexagonally flowered, nanowires, nanotubes, nanoneedles, and nanorods. Among these, spherically shaped SeNPs are more commonly employed for pharmacological and biological applications [53].

Nanocarriers have brought about a revolutionary impact on theragnostics and have emerged as a versatile platform for drug delivery. Their small size range (less than 200 nm) provides several advantages, such as improved interaction with Aβ fibrils, increased solubility in aqueous media, and enhanced intracellular permeability. Se NPs, with their high surface-to-volume ratios, have garnered considerable attention in the field of nano delivery [63].

Mesoporous selenium nanoparticles (MSeNPs), featuring pores ranging from 2 to 50 nm, exhibit remarkable characteristics, including a high surface area, low-density nanocarriers, and high volume for drug loading in drug delivery systems [33]. For example, Sun et al., demonstrated that borneol-loaded MSeNPs effectively crossed the BBB and released at the lesion site. The MSeNPs exhibited inhibitory effects on the aggregation of amyloid-Aβ proteins, alleviated oxidative stress, and suppressed tau hyperphosphorylation. Additionally, they provided protection to nerve cells and showed improvements in memory impairment in APP/PS1 mice [64].

Studies have also indicated that enlarging the size of NPs can lead to a decrease in their brain accumulation percentage and diminish their biological activities. Consequently, the relatively large size of SeNPs might render them unsuitable for the treatment of nervous system diseases [65].

Quantum dots (QDs) show immense promise as a novel nanodrug material due to their small size, good solubility, and large specific surface area. Numerous studies have highlighted their excellent biocompatibility, cost-effectiveness, and controllable fluorescence properties.

Their small size also facilitates BBB penetration, making them suitable for AD treatment. Additionally, their fluorescence characteristics, including high intensity, long life, and strong light stability, make QDs highly valuable in biological diagnosis and tracking detection in medical research. Guo et al., successfully developed efficient and straightforward ultrasmall-sized SeQDs with potent free-radical scavenging activity, effectively shielding cells from oxidative stress induced by various stimuli. This led to the inhibition of Aβ aggregation and significant reduction of Aβ-mediated cytotoxicity. Consequently, using SeQDs in AD treatment offers substantial advantages compared to traditional single-target drugs and opens new avenues for combining prevention and treatment in neurodegenerative diseases [66].

With the aim of creating multifunctional nanocomposites with small size and high biocompatibility for AD therapy, selenium-doped carbon quantum dots (SeCQDs) have been synthesized through a straightforward hydrothermal treatment of selenocystine. These SeCQDs demonstrated dual capabilities as they effectively inhibited Aβ aggregation and efficiently scavenged ROS produced in the brain. Zhou et al., introduced large amino acid mimicking SeCQDs as innovative nano agents for multi-target therapy in AD, owing to their capability to inhibit Aβ aggregation and their broad-spectrum antioxidant properties. The versatility of SeCQDs in functionalization and potential to cross the BBB position them as promising candidates for prospective nanodrugs for treating AD [65].

NPs morphology also plays a crucial role in the pharmacokinetics and cellular uptake of smart drug delivery systems. The design of an optimized nano drug delivery platform aims to achieve efficient delivery to the targeted site while minimizing off-target effects. Nano-spherical structures possess desirable properties, making them ideal shapes for nanoparticle vectors in therapy. They offer advantages such as high drug-loading capacity, prolonged circulation time, and enhanced cellular uptake [33].

2.3. Synthesis methods of Se-based nanoparticles

Due to their distinct surface activity and particle dispersion, SeNPs present numerous advantages compared to bulk selenium-based materials. These advantages include larger biological activity, higher catalytic efficacy, greater bioavailability, and lower toxicity [67].

SeNPs can be synthesized via chemical, physical and biological methods. Chemical synthesis involves the use of highly reactive chemicals, posing potential risks to human life and the environment. The process often requires elevated temperatures, dangerous chemicals, and an acidic pH for the catalytic reduction of ionic selenium, making it a less safe method for SeNPs synthesis [53].

In chemical methods, a selenium salt (commonly sodium selenite) serves as the precursor and source of Se. Additional precursors required for this wet chemical synthesis include reducing agents, templates, and capping agents. Reducing agents such as cetyltrimethylammonium bromide, ascorbic acid, and glutathione play a vital role in transforming the selenite ion into elemental Se in a zerovalent state. Chandramohan et al., conducted a study where different shapes of SeNPs (rod, sphere, and cube) were synthesized using various reducing agents such as bovine serum albumin, D-glucose, and soluble starch (amylum), respectively. This highlights the significance and influence of reducing agents on the shape of SeNPs [33].

Gholamigeravand et al., employed the chemical precipitation method to synthesize SeNPs. They added selenium powder to a solution of sodium sulphite, resulting in a transparent Na_2SeSO_3 solution used as a precursor for SeNPs synthesis. To confirm the formation of SeNPs, acetic acid was added until the solution turned pink. NPs obtained through this process demonstrated the ability to enhance memory impairment in streptozotocin-treated rats by increasing antioxidant capacity [68].

On the other hand, nanoparticle stability is a significant concern for their practical application, as NPs tend to agglomerate. One straightforward method to stabilize NPs is by coating them with a single layer of polymer or surfactant. This dense matrix increases viscosity and reduces the interaction between NPs, effectively inhibiting agglomeration. Coating not only protects NPs but also facilitates their conjugation with biomacromolecules. To stabilize SeNPs, various coating agents such as polymers, surfactants, or biocompatible substances have been utilized. Moreover, the concentration of the stabilizer plays a crucial role in determining the size and uniformity of the SeNPs [52].

In their study, Firouzi et al., employed polyvinyl alcohol (PVA) as a coating agent to synthesize coated SeNPs (PVA-SeNPs), and they assessed their effects in a rat model of AD. PVA, being a low-cost and non-hazardous organic polymer with good water solubility, increased the stability of SeNPs and improved their circulation time and drug loading capacity. The obtained results demonstrated that PVA-SeNPs effectively mitigated oxidative stress and memory impairment caused by streptozotocin neurotoxicity [69].

Polysaccharides offer several advantages as stabilizing agents, including the presence of multiple functional groups, biodegradability, and biocompatibility. SeNPs have been reported to be stabilized using polysaccharides such as guar gum, chitosan, malt dextrose, and hyaluronic acid. These polysaccharides are easily digested by enzymes within the body and do not pose any toxicity concerns.

Saini et al., utilized a three-step method involving the redox reaction of sodium selenite and ascorbic acid to synthesize SeNPs. To enhance the stability of the nanocarriers, xanthan gum powder was added. The synthesized NPs demonstrated promise for potential use in intervening in Aβ-induced cytotoxicity in neuronal cells [63].

Chitosan is one of the most commonly used polysaccharide coatings due to its non-toxic, biodegradable, and biocompatible properties. This linear biopolymer stabilizes NPs by virtue of its polycationic nature and conformation in solution, effectively increasing their stability during lyophilization. Despite the potential for a medium with high ionic strength to screen charges on the surface of NPs, leading to reduced solubility and increased aggregation, chitosan's electrostatic repulsion of negative charges on the nanoparticle surface promotes a stable suspension. Asl et al., employed chitosan-coated selenium nanoparticles to enhance the efficiency of stem cells in the neuroprotection of streptozotocin-induced neurotoxicity in adult male rats by increasing the antioxidant capacity [70].

On the other hand, Vicente-Zurdo et al., developed chitosan-coated selenium nanoparticles that demonstrated remarkable inhibition of metal-induced Aβ aggregation. Additionally, these NPs displayed a significant capacity to disaggregate Aβ fibrils, irrespective of the presence or absence of biometals. In the presence of Zn(II), the chitosan-coated selenium nanoparticles effectively reduced the length and width of the generated Aβ fibrils [71]. These SeNPs coated with the chiral stabilizing agent chitosan, exhibited a remarkable capability to reduce and even completely inhibit $A\beta_{42}$ aggregation induced in the presence of amino acid enantiomers associated with AD (D-Phe, D-Ala, D-Glu, D-Asp, and DL-SeMet). Furthermore, the study revealed that the chirality of these enantiomers influences the width of the amyloid fibrils [72]. Additionally, chitosan-coated selenium nanoparticles were evaluated *in vitro* using mouse (Neuro-2a) and human (SH-SY5Y) neuroblastoma cell lines demonstrating their potential to adhere and cross the cell membrane of neuroblastoma cells [73].

Other strategies to stabilize the SeNPs include proteins, polyphenols, and polysaccharides. However, polyphenols possess certain limitations, such as their tendency to undergo auto-oxidation at acidic pH and their propensity to aggregate [63].

Zhang et al., employed epigallocatechin-3-gallate, the primary polyphenol found in green tea, to stabilize SeNPs. These NPs were further coated with Tet-1 peptide, leading to a potent inhibition of Aβ fibrillation and efficient disaggregation of preformed Aβ fibrils into non-toxic aggregates [74].

Yang et al., utilized the polyphenol chlorogenic acid (CGA) to create CGA@SeNPs. These nanocomposites exhibited enhanced inhibition of

$A\beta_{40}$ aggregation and effectively protected PC12 cells from Aβ aggregation-induced cell death. The researchers found that CGA@SeNPs demonstrated greater efficiency in reducing $A\beta_{40}$ toxicity during long-term use compared to CGA alone [62]. While Vicente-Zurdo et al., synthetized chitosan-CGA@SeNPs, combining the biocompatibility of chitosan with the antioxidative and metal-chelating properties of selenium and chlorogenic acid. These SeNPs demonstrated remarkable metal interaction capabilities and excellent antioxidant properties, making them potentially effective scavengers of ROS—an essential aspect in addressing AD [71].

Yang et al., also coated SeNPs with the natural polyphenol dihydromyricetin (DMY) to create DMY@SeNPs. Subsequently, they stepwise decorated the DMY@SeNPs with chitosan to obtain CS/DMY@SeNPs, and further modified them with the BBB-targeting peptide TGN (TGNYKALHPHNG) to produce TGN-CS/DMY@SeNPs. These TGN-CS/DMY@SeNPs significantly reduced Aβ aggregation and exhibited enhanced anti-inflammatory effects of SeNPs *in vitro*. Moreover, both types of NPs were effective in repairing the gut barrier and regulating the population of inflammatory-related gut microbiota, including *Bifidobacterium*, *Dubosiella*, and *Desulfovibrio* [75].

In order to reduce surface free energy, smaller particles have a tendency to aggregate and merge into larger particles. Therefore, the use of a capping agent is crucial to provide stability to the NPs [63]. Capping agents primarily consist of various carbohydrates or chemical groups, and they play a significant role in regulating the dispersion of NPs [52]. Thus, Sun et al., produced chiral penicillamine-capped SeNPs (L-/D-Pen@SeNPs) that function as a novel class of chiral amyloid-Aβ inhibitors. These NPs exhibited higher inhibition efficiency compared to D-Pen@SeNPs and also showed promising effects in ameliorating cognition and memory impairments [76].

The majority of the mentioned SeNPs synthesis methods involve chemical reduction techniques, which could pose challenges in their biological applications due to the use of toxic reducing and capping agents.

SeNPs synthesis can be also done from physical methods such as phyto-thermal associated synthesis, γ-irradiation, lithography, pyrolysis, pulsed laser ablation, sonochemical, ultrasonic, microwave-assisted, ionic liquid-induced, electrodeposition or chemical vapor deposition. In a study, SeNPs were synthesized using the ionic liquid-induced method, wherein stabilizers such as polyvinyl alcohol, sodium dodecyl sulphate, polysorbate 80, or tryptone were added. Another electrochemical method involved maintaining the reaction at 130 °C and incorporating sodium dodecyl sulphate and cetane trimethyl ammonium bromide for SeNPs modifications [35].

Regarding to γ-rays, water-stable SeNPs were produced using several natural macromolecules. Additionally, SeNPs were synthesized by pulsed laser ablation by irradiating selenium pellets. Selenium nanomaterials were also prepared by a microwave approach with L-asparagine and H_2SeO_3, as well as with selenium tetrachloride as the precursor under microwave irradiation [67].

However, these alternative physical methods are less commonly utilized than chemical methods [53] and may not be as popular in the SeNPs synthesis process. However, they do offer some control over the size and shape of the NPs by manipulating the physical and mechanical properties of the method [33].

The physical method requires the use of expensive equipment for synthesis, involving extreme pressure or temperatures. On the other hand, chemical techniques entail multiple steps with the utilization of hazardous reagents. Therefore, in comparison to the biosynthesis of NPs, both chemical and physical techniques are costly and can be environmentally toxic [35].

Alternatively, biological methods, also known as green methods, have been reported for the synthesis of SeNPs. They offer a promising approach to develop reliable, non-toxic, and eco-friendly techniques for nanoparticle synthesis. These methods also involve the employment of phytochemicals from plant sources or proteins from microbes as reducing and stabilizing agents, which are cost-effective, abundantly available, and environmentally safe. Additionally, green synthesis can be conducted at room temperature without the need for external stimuli, expensive equipment, or extreme pressure or elevated temperatures [35].

Biological methods employing algae, yeast, fungi, and plants as biological catalysts for nanoparticle production are highly effective. These methods offer several advantages over chemical and physical approaches, including lower cost, rapid growth rates of microorganisms and plants, reduced toxicity, standard culturing procedures, absence of severe extreme conditions, and eco-friendly nanoparticle production. The biosynthesis of SeNPs has been conducted using various plant extracts, i.e., *Cinnamomum zeylanicum* bark, fresh citrus and lemon fruits, *Aloe vera* leaf extracts, *Dillenia indica*, *Vitis vinifera*, *Prunus amygdalus* leaf or *Allium sativum* [53]. The primary advantage of using plant extracts is that the plant secondary metabolites serve as natural reductants and stabilizing agents, making it an environmentally friendly approach.

SeNPs derived from *Rosmarinus officinalis* and *Abelmoschus esculentus* are other examples of SeNPs biological synthesis with plant extracts [33]. Al-Qaraleh et al., also synthetized SeNPs using *Moringa peregrina* leaves extract, which showed a considerable antioxidant potential [77].

On the other hand, Borowska et al., developed a novel microwave-assisted green synthesis of high stable SeNPs using yeast extract as source of non-toxic reducing and capping agents [78]. González-Salitre et al., fabricated SeNPs by using the probiotic yeast *Saccharomyces boulardii*, which exhibited a wide range particle size distribution [79].

Certain studies have also used green sources like *Bacillus mycoides*, *Clostridium Perfringens*, *Saccharomyces cerevisiae*, *Zooglea ramigera* and dried *Vitis vinifera* (raisin) extract as reducing agents, that also contribute to stabilizing the SeNPs integrity and structure [35]. In the study conducted by Bulgarini et al., SeNPs were produced by the help of five different bacterial species [33], while Qiao et al., prepared biogenic SeNPs by *Lactobacillus casei* ATCC 393 (*L. casei* ATCC 393), which exhibited significant antioxidant and anti-inflammatory activities *in vitro* and *in vivo* and effectively alleviated the $A\beta_{25-35}$-induced toxicity in PC12 cells via Akt/CREB/BDNF signaling pathway [80].

However, bacterial synthesis typically involves longer processing times compared to chemical and physical methods. Additionally, there are additional steps required for the purification of SeNPs, resulting in NPs that are often non-uniform in size and have a broad size range [81].

Therefore, while green synthesis is considered less toxic and cost-effective, its reproducibility remains a significant challenge. As mentioned above, several methods have been described to produce SeNPs using a wide variety of precursors, reducing agents and stabilizers, plant extracts and/or microorganisms. Table 1 summarizes some of the procedures used for the chemical synthesis of SeNPs involved in Alzheimer's disease studies, while Table 2 includes some examples of biogenic and green SeNPs synthesis methods.

2.4. Encapsulation of selenium nanoparticles

The variation in size and bioactivity of pH-sensitive SeNPs has prompted researchers to explore nano-sized encapsulation systems extensively. Stimuli-sensitive drug delivery, aiming for on-demand drug release, is a promising strategy. Targeted release based on pH variation has gained significant attention in this context.

The encapsulation of nanomaterials using hydrophobic and hydrophilic substrates offers a way to modify pharmacokinetics, allowing for realistic strategies to control circulation through the reticuloendothelial system after cellular uptake. In the development of nanoparticle-based diagnostic/therapeutic agents and food supplements, innovative approaches are crucial to achieve *in vivo* target-specific retention, endosome escape, and clearance through various mechanisms. These factors play pivotal roles in the successful application of nanotechnology in biomedicine and various life science applications [52].

To mitigate Aβ-induced neuronal cytotoxicity, SeNPs and silymarin

Table 1
Chemical synthesis of SeNPs used in Alzheimer's disease studies.

Precursor	Reducing agent	Stabilizer/Decorator	Particle size (nm)	Zeta potential (mV)	Characterization techniques	Observations	Reference
Na_2SeO_3	Vitamin C	Polyvinyl pyrrolidone/ resveratrol	8.00 ± 0.34	−10.31 ± 1.17	TEM, UV–Vis and FTIR spectroscopy, DLS, fluorescence	Simple layer-by-layer structure. Homogeneous and nearly spherical structure.	[57]
Na_2SeO_3	Vitamin C	Polyvinyl pyrrolidone/ resveratrol and TGN peptide	14.00 ± 0.12	−6.01 ± 0.39	TEM, UV–Vis and FTIR spectroscopy, DLS, fluorescence	Simple layer-by-layer structure. Homogeneous and nearly spherical structure.	[57]
Na_2SeO_3	$NaBH_4$	Resveratrol	~100		TEM and HR-TEM, UV–Vis and FTIR spectroscopy, DLS, RLS, fluorescence	Spherical structure and amorphous coating layer.	[55]
Na_2SeO_3		Resveratrol	60–90		TEM, UV–Vis and FTIR spectroscopy, DLS	Spherical shape.	[56]
Na_2SeSO_3	Glacial acetic acid	Polyvinyl alcohol			SEM, EDX, FTIR	Se powder was dissolved in Na_2SeO_3 solution to obtain a transparent Na_2SeSO_3 solution, which was used as precursor. Spherical and uniform structure.	[69]
Na_2SeSO_3	Acetic acid		<50 nm		TEM, XRD, TFIR, MTT assay	Se powder was dissolved in Na_2SeO_3 solution to obtain a transparent Na_2SeSO_3 solution, which was used as precursor. Se only and nano-crystalline NPs. Monodisperse spherical structure.	[61]
H_2SeO_3	Ascorbic acid	Polyethylene glycol			DLS, TEM, SEM, XRD, FTIR		[82]
H_2SeO_3	Ascorbic acid	Polyethylene glycol/ curcumin-poly-lactide-*co*-glycolide polymer	160 ± 5 (DLS) 71 ± 6 (TEM & SEM)		DLS, TEM, SEM, XRD, FTIR	Spherical shaped structure.	[82]
Na_2SeO_3	Ascorbic acid	Xanthan gum powder	119 ± 3 and 253 ± 3 range	−35.4 ± 3.8 and −43.3 ± 2.4 range	HR-TEM, DLS, UV–Vis and FTIR spectroscopy, DSC, XRD, DPPH scavenging method and MTT assay	Smooth, regular, and spherical in shape appearance. Amorphous nature and segregated particles.	[63]
Na_2SeO_3	L-cys	Chondroitin sulphate	89.1 ± 4.5	−41.7 ± 3.5	DLS, TEM, FTIR	Monodispersed and homogeneously spherical structure.	[34]
Na_2SeSO_3	Acetic acid	Chitosan	30 ± 20		SEM, EDX, FTIR, MTT assay	Spherical shape.	[70]
Na_2SeO_3	Ascorbic acid	Polyvinyl pyrrolidone/ polydopamine-borneol	160	−12.7	TEM, SEM, EDX, FTIR	Spherical morphology.	[83]
Na_2SeO_3		Acacia and polysorbate 80/Quercetin	90 ± 4	−9.9 ± 0.5	DLS, SEM, UV–Vis and FTIR spectroscopy, DPPH scavenging method	Homogeneous nanocomposites.	[84]
Na_2SeO_3	Vitamin C	Polyvinyl pyrrolidone/ chlorogenic acid	~7.52	−15.2 ± 0.2	TEM, UV–Vis and FTIR spectroscopy, DLS, fluorescence		[85]
Na_2SeO_3	Vitamin C	Polyvinyl pyrrolidone/ chlorogenic acid and TGN peptide	9.43	−11.4 ± 0.5	TEM, UV–Vis and FTIR spectroscopy, DLS, fluorescence		[85]
Na_2SeO_3	$NaBH_4$	Chlorogenic acid	~100		TEM, EDX, UV–Vis and FTIR spectroscopy, DLS, fluorescence	Spherical structure.	[62]
Na_2SeO_3	$NaBH_4$	D- and L-penicillamine (Pen)	L-Pen SeNPs ~ 88.1 D-Pen SeNPs ~113.5	L-Pen SeNPs −8.36 D-Pen SeNPs −6.93	TEM, DLS	Monodispersion and homogeneous spherical shapes.	[76]
Na_2SeO_3	Ascorbic acid	Chitosan dissolved in 3 % of acetic acid	60 ± 6	−38 ± 1	TEM, DLS, EDXS, ED, DPPH scavenging assay	Spherical morphology and crystal structure.	[71]
Na_2SeO_3	Ascorbic acid	Chitosan dissolved in 3 % of acetic acid/ chlorogenic acid	80 ± 20	45 ± 1	TEM, DLS, EDXS, ED, DPPH scavenging assay	Spherical morphology and crystal structure.	[71]

were incorporated into a single polysaccharide matrix (xanthan gum) to provide dual antioxidant and Aβ fibril disaggregation capabilities. Silymarin, a plant-based therapeutic agent known for its neuroprotective properties, effectively inhibits Aβ fibril formation in neuronal cells. Xanthan gum, on the other hand, serves as a readily available biocompatible and biodegradable stabilizer commonly used in the food and pharmaceutical industry. It has also been listed in the FDA's inactive ingredient database. The NPs were designed to alleviate amyloid-induced cytotoxicity in SH-SY5Y cells. These nanocarriers demonstrated anti-aggregation properties in neuronal cell lines and effectively reduced Aβ-induced cytotoxicity, highlighting their potential for neuroprotection and therapeutic applications in Alzheimer's disease [63].

Selenium nanocomposites (SeNCs) have also been synthesized to enhance the bioavailability of bioactive molecules and serve as a simple strategy for drug delivery. For instance, Qia et al., developed P80-Que@SeNC to enhance the bioavailability of quercetin (Que), a flavonoid antioxidant widely used to inhibit Aβ fibril formation and potentially reduce oxidative stress. Que's limited aqueous solubility, extensive first-pass metabolism, and low BBB permeability hinder its clinical application. The authors combined Que and Na_2SeO_3 to produce SeNPs, which were subsequently modified using a combination of acacia and

Table 2
Green synthesis of SeNPs which could be exploited potential further for pharmaceutical and/or biomedicine applications.

Precursor	Extract origin/Microorganism	Particle size (nm)	Characterization techniques	Observations	Reference
Selenium oxyanions	*Sulfurospirillum barnesii, Bacillus selenitireducens, Selenihalanaerobacter shriftii*	~300	UV–Vis absorption and Raman spectra	Monoclinic crystalline structures	[86]
Na_2SeO_3	*E. Coli* K-12	10-90 (TEM) 60 ± 20 (DLS)	TEM, SEM, EDXS, DLS, UV–Vis spectroscopy	Spheroidal particles with no crystalline structure.	[87]
Se_2Cl_2	*Klebsiella pneumonia*	100-550 (250 ± 80)	TEM, UV–Vis spectroscopy, EDS		[88]
$HNaO_3Se$	*Lactobacillus casei, Lactobacillus acidophilus, Bifidobacterium, Klebsiella pneumonia*	50–500 50–500 400–500 100–550	TEM, UV–Vis spectroscopy	Production time 12–48 h. Homogeneous particle size distribution and regular, spherical shape.	[89]
H_2SeO_3	Dried *Vitis vinifera* (raisin) extract	3-18 (TEM) 8 ± 3 (DLS)	TEM, DLS, XRD, EDX and FTIR spectroscopy	Crystalline nature and spherical shape.	[90]
H_2SeO_3 and ascorbic acid	Fenugreek seed extract	50–150	UV–Vis and FTIR spectroscopy, SEM, DLS, XRD, elemental analysis by X-ray fluorescence	Nanocrystalline in nature. The reduction of selenious acid was attributed to the presence of polysaccharide galactomannan, abundant in fenugreek seeds.	[91]
Na_2SeO_3	*Terminalia arjuna* leaf extract	10–80	UV–Vis and FTIR spectroscopy, TEM, EDX, XRD	Polydispersed and crystalline NPs.	[92]
Na_2SO_3	*Moringa peregrina* leaves extract	80–150	FTIR, XRD, SEM, DLS, EDX, DPPH assay	Agglomerated spheres with smooth surfaces and negative electric charges on their surfaces.	[77]
SeO_2 with NaOH	Yeast extract	<200	Single particle ICP-MS, scanning TEM	Microwave-assisted synthesis. Spherical particles.	[78]
Na_2SO_3	*Saccharomyces boulardii*	365–25150	TEM	Spherical morphology	[79]

polysorbate 80. The newly developed P80-Que@SeNC demonstrated improved drug delivery across the BBB, facilitated by the presence of polysorbate 80, which acts as a pharmaceutical excipient enhancing the aqueous solubility of quercetin. In vitro experiments showed that P80-Que@Se exhibited higher aqueous solubility compared to individual Que, effectively inhibiting Aβ fibrillation, suggesting its potential as a therapeutic drug candidate. Furthermore, P80-Que@SeNC exhibited strong 1,1-diphenyl-2-picrylhydrazyl (DPPH) radical scavenging activity, indicating excellent antioxidant properties [84].

A nano formulation of curcumin (Cur) for AD therapeutics was developed by modifying the surface of the poly-lactide-*co*-glycolide (PLGA) polymer and encapsulating SeNPs. Huo et al., utilized the emulsion solvent evaporation process to prepare SeNPs loaded Cur/PLGA composites. The drug delivery system of Cur-loaded Se-PLGA nanospheres showed promising results, reducing amyloid-β load in the brains of AD mice and significantly improving memory deficiency in the model mice. This approach could be an effective treatment for Alzheimer's disease [82].

On the other hand, a novel flowerlike selenium nanocluster (TGN-CGA@SeNCs) was developed using the brain-targeting peptide (TGN peptide) and CGA. This nanocluster aimed to enhance the bioavailability of CGA, a common dietary polyphenol known for its neuroprotective effects. Both CGA-modified selenium nanocluster (CGA@SeNCs) and TGN-CGA@SeNCs demonstrated improved efficacy in ameliorating gut microbiota disorder at the same concentration. Particularly, TGN-CGA@SeNCs significantly increased the relative abundance of *Turicibacter*, *Colidextribacter*, *Ruminococcus*, *Alloprevotella,* and *Alistipes*, which are associated with reducing oxidative stress, inflammation, and glucose homeostasis imbalance. Furthermore, TGN-CGA@SeNCs showed the capability to transport through the BBB, surpassing the effects of CGA@SeNCs in regulating Aβ aggregation and enhancing brain glucose homeostasis [85].

2.5. Techniques used for selenium nanoparticles characterization

For the translation of Se-based nanotechnology into clinical applications, it is essential to not only establish safe, simple, sustainable, and cost-effective methods for SeNPs synthesis but also gain a comprehensive understanding of their relevant physicochemical and biological properties [67].

SeNPs are usually characterized using microscopic and spectroscopic methods. The morphology and particle size distribution of NPs are usually characterized by transmission electron microscopy (TEM) and scanning electron microscope (SEM) (Tables 1 and 2). The morphological characterization is of great interest because morphology always influences most of the properties of the nanoparticle. Therefore, several authors and researchers investigate the size and shape of the synthesized SeNPs by both types of electron microscopy [93]. TEM with energy-dispersive X-ray (EDX) also provides micrographs showing the size and surface morphology of the SeNPs, as it is shown for SeNPs stabilized with CGA (CGA@SeNPs) in Fig. 2 a [71]. Therefore, to further confirm the presence of Se in the NPs, EDX spectra can be used, since this technique allows to identify the composition of the synthesized nanomaterials [62,69–71,83].

On the other hand, the surface composition and the functional groups of prepared NPs is frequently analyzed by using UV–Vis and Fourier transform infrared (FTIR) spectroscopy (Tables 1 and 2), and in some case, by a fluorescence spectrophotometer [55,57,62,85]. FTIR spectroscopy is a non-destructive analytical technique used for the characterization of organic and inorganic materials to investigate functional groups linked to the compounds. It is also used to study the physical state and chemical composition of the sample [93].

Particle size, zeta potential, and the polydispersity index of fabricated SeNPs can be also determined using dynamic light scattering (DLS) (Fig. 2d) [34,55–57,62,71,76,82,84,85]. The stability of SeNPs under physiological conditions, and consequently the kinetics of their decomposition, depends on numerous factors. Among the most critical are their size (larger particles have a greater surface area in contact with the environment, leading to a higher decomposition rate but a longer time until particle breakdown), stabilizing agent (which maintains colloidal stability and prevents particle agglomeration or precipitation), surface modifications (enhancing reactivity with specific targets related to AD but simultaneously promoting interaction with the environment), and, of course, the core of the nanoparticles.

However, the primary parameter for characterizing nanoparticle stability is the zeta potential (ZP), defined as the potential with which colloidal particles move under an electric field. The ZP provides information about the nanoparticles' stability against agglomeration, categorizing them as highly unstable ($|ZP| < 10$ mV), relatively stable (10

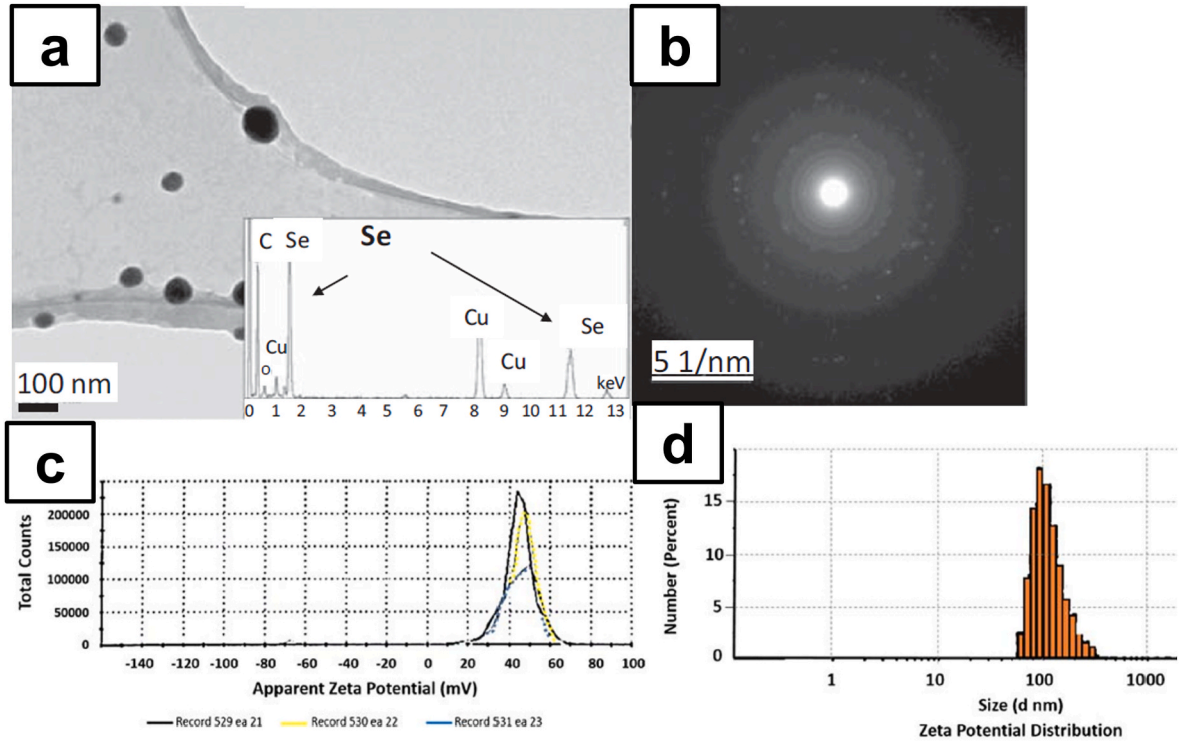

Fig. 2. Characterization of CGA@SeNPs employing TEM and EDX (a), electron diffraction pattern (b), DLS (c) and ZP (d) graphs. Adaptation from Vicente-Zurdo, D. et al. [71].

mV < |ZP| < 20 mV), moderately stable (20 mV < |ZP| < 30 mV), and highly stable (|ZP| > 30 mV). An example of ZP graph is shown in Fig. 2 c for CGA@SeNPs.

On the other hand, the employment of X-ray diffraction (XRD) allows to determine the crystalline or amorphous nature of the synthetized SeNPs. To assess their crystal morphology, the lyophilized powder of the samples or the finely ground and homogenized sample is used and detected by monochromatic X-rays [61,63,82]. The content of Se in Se-NPs has also been determined by inductively coupled plasma (ICP) emission spectroscopy [83]. Differential Scanning Calorimeter (DSC) have been employed for thermal analysis of SeNPs, although this technique has been scarcely used [63].

Regarding biological properties, resonance light scattering (RLS) has been employed, for example, to study the binding affinity of resveratrol-SeNPs for $A\beta_{42}$ [55] and MTT assay has been used to determine the cytotoxicity of Se-NPs [61,63,70].

However, cellular uptake and accumulation of NPs are important parameters to determine their effect in living organisms. TEM may be useful to provide information on the pathway of these NPs in their internalization by cells, but it does not provide quantitative information about the concentration of NPs inside a single cell. With this purpose, single cell-ICP-MS have been used by few authors to obtain quantitative results of bioaccumulation at trace level [73,78]. Finally, the DPPH scavenging method is usually employed for evaluate the antioxidant properties of SeNPs [63,71,77,84].

3. SeNPs and their role in AD treatment: *in vitro* studies

In recent years, nanotechnology has emerged as a promising field for the development of innovative therapeutic strategies in the treatment of neurodegenerative disorders, including AD. Among the various nanomaterials investigated, SeNPs have gained significant attention due to their unique physicochemical properties and potential therapeutic applications. *In vitro* studies focusing on SeNPs have provided valuable insights into their role in AD treatment, particularly concerning their interactions with Aβ protein and their potential neuroprotective effects [53].

SeNPs showcase a remarkable spectrum of bioactive properties, thanks to their diverse synthesis methods and functionalization approaches. Among these properties, their antioxidant and anti-inflammatory capacities stand out, offering potential benefits across a range of neurodegenerative diseases. However, it is in the treatment of AD that their distinctive value becomes most apparent.

The tailored application of SeNPs against specific targets implicated in the pathogenesis of AD distinguishes their therapeutic potential. Notably, SeNPs have demonstrated efficacy in inhibiting beta-amyloid aggregation and mitigating the hyperphosphorylation of tau protein. These targeted actions position SeNPs as potential disruptors of the cascade of events outlined in the amyloid cascade hypothesis, which is considered a pivotal driver in the development of AD.

Beyond their general bioactive properties, the capacity of SeNPs to intervene at key molecular levels associated with AD pathology marks them as promising candidates for therapeutic interventions. By addressing multiple facets of AD, from oxidative stress and inflammation to specific protein abnormalities, SeNPs hold the potential to not only ameliorate symptoms but also modify the underlying disease processes.

As research progresses, further elucidation of the nuanced interactions between SeNPs and AD-specific molecular targets may uncover additional avenues for intervention. This underscores the importance of ongoing investigations into the intricate mechanisms through which SeNPs exert their effects, offering a pathway towards innovative and targeted approaches in the quest for effective AD treatments.

This section aims to provide a comprehensive overview of the findings from in *vitro* studies investigating SeNPs in the context of AD. By examining the chemical interactions between SeNPs and $A\beta_{42}$ and evaluating their neuroprotective effects using cell models, a deeper understanding of the therapeutic potential of SeNPs in AD may be achieved.

The investigation of the chemical interactions between SeNPs and

$A\beta_{42}$ forms a critical aspect of this review. Various bioanalytical techniques have been employed to assess the binding affinity, kinetics, and conformational changes occurring during the SeNPs-$A\beta_{42}$ interaction. These techniques, including spectroscopic and microscopic analyses, have provided valuable insights into the ability of SeNPs to modulate Aβ aggregation and potentially mitigate its neurotoxic effects [94].

Additionally, the evaluation of the neuroprotective effects of SeNPs using cell models has further contributed to our understanding of their potential as therapeutic agents for AD. By employing different cell lines commonly studied in AD field, researchers have assessed the protective effects of SeNPs against Aβ-induced neurotoxicity. Various experimental techniques, such as cell viability assays, antioxidant determination and immunofluorescence staining, have been employed to investigate the underlying cellular mechanisms and signaling pathways involved in the neuroprotective effects of SeNPs [70].

Through these *in vitro* studies, significant progress has been made in unravelling the potential of SeNPs as therapeutic interventions for AD. Further exploration of SeNPs in preclinical and clinical studies holds great promise for advancing our understanding of their therapeutic efficacy and potential translation into effective treatments for AD, providing hope for improved outcomes in the management of this devastating neurodegenerative disorder.

3.1. Exploring chemical interactions between selenium nanoparticles and $A\beta_{42}$: an integrated approach through diverse bioanalytical techniques

The chemical interaction between Se or SeNPs and biomolecules involves intricate processes determined by factors such as the selenium form, NPs size, surface characteristics, and the nature of biomolecules. SeNPs possess functional groups on their surface that facilitate interaction with biomolecules through mechanisms like hydrogen bonding, van der Waals forces, and electrostatic interactions. Due to its redox activity, SeNPs participate in redox reactions in biological environments, impacting cellular redox balance.

Proteins can bind to SeNPs through surface adsorption or covalent bonds with amino acid residues, potentially altering protein

Table 3
Compendium of the principal methods and analytical techniques for investigating the effect of SeNPs on the $A\beta_{42}$ protein.

Method/Technique	Experimental conditions						Reference
ThT/Fluorescence spectroscopy	***Medium***	***Incubation time***	***ThT (μM)***	***Darkness (min)***	***Excitation/emission wavelength (nm)***	***Aβ (μM)***	
	50 mM PBS	0–5 days	15	15	440/490	35	[55]
	10 mM Tris-HCl	1–11 days	20	10	440/480	25–50	[80]
	10 mM Tris, 150 mM NaCl	0–7 days	10	*Not specified*	444/482	100	[65]
	10 mM PBS, 10 mM Na_2HPO_4, 10 mM NaH_2PO_4	0–60 min	*Not specified*	*Not specified*	440/488	20 (mM)	[76]
	50 mM PBS	0–5 days	15	*Not specified*	440/490	35	[62]
	10 mM PBS	3 days (100 rpm)	10	*Not specified*	*Not specified*/480	20	[74]
	DMEM	3 days	25	*Not specified*	440/480	100	[34]
ANS/Fluorescence spectroscopy	***Medium***	***Incubation time***	***ANS (μM)***	***Darkness (min)***	***Excitation/emission wavelength (nm)***	***Aβ (μM)***	
	Not specified	3 days	50	30	380/500	30	[34]
Congo red/UV–Vis spectroscopy	***Medium***	***Incubation time***	***Congo red (μM)***	***Darkness (min)***	***Absorption wavelength (nm)***	***Aβ (μM)***	
	20 mM PBS, 50 mM NaCl	3 days	30	30	500	30	[34]
Transmission Electron Microscopy (TEM)	***Medium***	***Incubation time***	***Voltage (kV)***		***Negative staining (%, w/v)***	***Aβ (μM)***	
	50 mM PBS	3 days	Not specified		Phosphotungstic acid (1.5)	35	[55]
	10 mM Tris, 150 mM NaCl	*Not specified*	200		Phosphotungstic acid (1.5)	100	[65]
	10 mM PBS, 10 mM Na_2HPO_4, 10 mM NaH_2PO_4	2 days	*Not specified*		Uranyl acetate (2)	*Not specified*	[76]
	50 mM PBS	3 days	*Not specified*		Phosphotungstic acid (1.5)	35	[62]
Method/Technique	***Medium***	***Incubation time***	***Voltage (kV)***		***Negative staining (%, w/v)***	***Aβ (μM)***	**Reference**
Transmission Electron Microscopy (TEM)	10 mM PBS	6–96 h (100 rpm)	80		Uranyl acetate (2)	20	[74]
	10 mM HCl	2 days	100		Uranyl acetate (2)	50	[71]
	10 mM HCl	2 days	100		Uranyl acetate (2)	50	[72]
	Not specified	3 days	*Not specified*		Phosphotungstic acid (2)	1 (mg mL^{-1})	[34]
Atomic Force Microscopy (AFM)	***Medium***				***Incubation time***	***Aβ (μM)***	
	10 mM PBS, 10 mM Na_2HPO_4, 10 mM NaH_2PO_4				2 days	*Not specified*	[76]
	10 mM PBS				6–96 h (100 rpm)	20	[74]
Resonance light scattering (RLS)/ Fluorescence spectroscopy	***Medium***		***Incubation time***		***Excitation/emission wavelength (nm)***	***Aβ (μM)***	
	H_2O		10 min		200-800/200-800	0.05-0.5	[55]
	H_2O		10 min		200-800/200-800	0.6	[62]
Nuclear Magnetic Resonance (NMR) spectroscopy	***Medium***			***Incubation time***		***Aβ (μM)***	
	HEPES/10 % D_2O			2 h		200	[65]
Circular dichroism (CD)	***Medium***			***Incubation time***	***Absorption wavelength (nm)***	***Aβ (μM)***	
	10 mM Tris, 150 mM NaCl			7 days	200–300	100	[65]
	10 mM PBS, 10 mM Na_2HPO_4, 10 mM NaH_2PO_4			2 days	190–260	10	[76]
	10 mM PBS			1–3 days	190–290	20	[74]
	DMEM			3 days	200–290	100	[34]

conformation and activity. SeNPs may also interact with enzymes, influencing their activity and, in the case of selenoproteins, modulating cellular functions. Interactions with nucleic acids, such as DNA and RNA, are possible, potentially affecting gene expression and genetic material integrity. Cellular uptake mechanisms, like endocytosis, facilitate the internalization of SeNPs, allowing interaction with intracellular biomolecules and influencing cellular signaling pathways.

The antioxidant properties of selenium, including SeNPs, involve scavenging free radicals and reactive oxygen species, offering cellular protection from oxidative damage. This diverse range of interactions underlines the complexity and potential applications of SeNPs in various fields, including medicine and nanotechnology.

The $A\beta_{42}$ protein is the keystone of current strategies in the development of drugs for the treatment of AD, as its aggregation is the initiator in the "amyloid cascade hypothesis", which is primarily responsible for the development of AD. As mentioned above, the events triggered by the aggregation of $A\beta_{42}$ into extracellular amyloid plaques include impairment of interneuronal synapses, decreased mitochondrial respiration in neurons and astrocytes, oxidative stress, neuroinflammation and the formation of intracellular tangles due to hyperphosphorylation of tau with consequent disruption of cellular metabolism in neurons [21].

Since $A\beta_{42}$ aggregation is the main cause of AD development, recent strategies are focused in inhibit the interaction between monomers, which lead to the formation of extracellular amyloid plaques. Different analytical methods and techniques, found in literature, to quantify and observe $A\beta_{42}$ aggregation are compilated in Table 3. These methods include molecular fluorescence using Thioflavin T (ThT), transmission electron microscopy (TEM), and RLS. These techniques provide valuable information about the aggregation process, fibril morphology, and protein-nanoparticle interactions. In this context, the use of SeNPs modified with polyphenols such as resveratrol, CGA, epigallocatechin-3-gallate (EGCG), chiral penicillamine, as well as biogenic SeNPs, has shown potential in inhibiting amyloid aggregation and protecting against AD-related toxicity. This section compiles and discusses the different techniques and methods used to study $A\beta_{42}$ aggregation and highlights the results obtained by employing SeNPs.

One of the most accurate techniques to quantify amyloid aggregation and evaluate the aggregation process is the molecular fluorescence employing ThT as intercalating agent. ThT intercalates between aggregated $A\beta_{42}$ fibrils, changing its structure and thus its excitation length from 415 nm in its free form to 450 nm in protein binding, with emission at 490 nm. This increase in ThT intensity at 490 nm, due to $A\beta_{42}$ aggregation, can be determined by fluorescence spectroscopy [95].

Microscopy techniques such as TEM can be used to assess the morphology of $A\beta_{42}$ protein aggregation [96]. Negative staining methods, such as the use of uranyl acetate or phosphotungstic acid, are necessary to observe these fibrils correctly. In addition, the microscope voltage should not be too high to avoid degradation of the organic matter. The micrographs obtained can be used to obtain data on the aggregation of the $A\beta_{42}$ protein under different conditions, and to estimate the length and width of the fibrils using programs such as ImageJ [97].

RLS is an optical technique that can provide information about the binding of $A\beta_{42}$ fibrils to NPs, due to its high sensitivity [75]. This technique provides information about the radius of the nanoparticle, thus confirming the modification of its surface due to possible protein interactions.

Resveratrol is a polyphenol with remarkable antioxidant properties, which has been used to modify SeNPs surface [55]. SeNPs stabilized with resveratrol (Res@SeNPs) were able to interact with $A\beta_{42}$ fibrils, as TEM analysis (experimental conditions shown in Table 3) revealed that fibrils bounded to the surface of the NPs, not observing free Res@SeNPs in the micrographs. By using RLS (Table 3), Res@SeNPs signal increased in presence of $A\beta_{42}$ fibrils, confirming the binding of the fibrils on the surface of the NPs via Se–N bonds. $A\beta_{42}$-Res@SeNPs binding could interfere with the “metal ion hypothesis”, preventing metal ions to interact with $A\beta_{42}$ fibrils. To this end, ThT assay (Table 3) was employed to study the kinetic of $A\beta_{42}$ fibrils aggregation, induced by Cu(II), during 5 days in presence of Res@SeNPs. Cu(II) increased ThT signal, obtaining a maximum at 48 h of incubation. Res@SeNPs were able to delay fibril aggregation up to 3 days. Res@SeNPs tested concentrations (20, 40 and 60 μg mL^{-1}) proved that inhibition of amyloid aggregation was dose-dependent, being ThT fluorescence minimum at higher concentrations of Res@SeNPs. Therefore, surface modification of SeNPs with resveratrol improves their antiamyloidogenic properties, blocking Cu(II) binding to $A\beta_{42}$ fibrils.

Another polyphenol with potential application in NPs surface functionalization is CGA [71]. CGA@SeNPs proved to reduce $A\beta_{40}$-induced H_2O_2 generation employing DCFH-DA method [62]. For this purpose, 35 μM $A\beta_{40}$ was incubated with various concentrations of CGA@SeNPs (20, 40 and 60 μg mL^{-1}) at 37 °C for 3 days. Afterwards, 100 μM DCFH-DA was added and fluorescence was recorded at 488 nm excitation and 525 nm emission wavelengths. CGA@SeNPs reduced H_2O_2 generation in a dose-dependent manner, from 60 % (20 μg mL^{-1}) to 70 % reduction (60 μg mL^{-1}). Inhibition of $A\beta_{40}$ fibrillation was evaluated by ThT assay for 5 days (conditions shown in Table 3). While $A\beta_{40}$ reached a plateau of fibrillation at 3 days of incubation with a maximum at 200 % of fluorescence intensity (compared to $t = 0$), in presence of CGA@SeNPs fluorescence intensity remained constant, specially at 60 μg mL^{-1}. Morphology of $A\beta_{40}$ fibrils was evaluated by TEM (conditions shown in Table 3). CGA@SeNPs results were consistent with ThT assay, preventing fibrils formation at 60 μg mL^{-1}. To deepen the interaction between $A\beta_{40}$ and CGA@SeNPs, RLS was applied (conditions shown in Table 3). Intensity of CGA@SeNPs incubated with $A\beta_{40}$ showed higher intensity (150 %) than CGA@SeNPs alone at 475 nm, confirming the binding of the amyloid protein to the surface of SeNPs by Se–N bonds. For that reason, CGA@SeNPs could interfere with $A\beta_{40}$ fibrillation since they were able to block contact between monomers during incubation.

Epigallocatechin-3-gallate (EGCG) is the most abundant polyphenol in green tea, with outstanding antioxidant properties. On this basis, EGCG has also been used to stabilize SeNPs (EGCG@SeNPs) [74]. However, EGCG has serious drawbacks, such as low cellular uptake, poor bioavailability, and cytotoxicity at high concentrations. To solve these problems, EGCG@SeNPs have been coated with Tet-1, a peptide of the tetanus toxin (Tet-1-EGCG@SeNPs). To evaluate the ability of these NPs to Aβ, ThT assay was employed (conditions shown in Table 3). While Aβ at 20 μM concentration generated a typical sigmoidal curve starting at 10 h of incubation with a maximum of 14000 a.u. at 70 h, in presence of 10 μg mL^{-1} of EGCG@SeNPs and Tet-1-EGCG@SeNPs the maximum level decreased to 5000 a.u. and 4000 a.u., starting at 30 h and 40 h, respectively. To observe fibrils morphology, TEM technique was applied (conditions in Table 3). The presence of SeNPs led to an increase in amorphous oligomers and short fibrils, in contrast to Aβ alone, where large fibrils were observed. Tet-1-EGCG@SeNPs produced smaller amorphous oligomers than those obtained by EGCG@SeNPs, revealing the potential neuroprotection of Tet-1 peptide against AD. AFM was employed to monitor fibrillation process (conditions shown in Table 3), corroborating the ability of both types of SeNPs to inhibit amyloid plaques. Both SeNPs were able to disaggregate preformed fibrils, by TEM and AFM measurements, at different paces. While Tet-1-EGCG@SeNPs started the disaggregation process at 24 h of incubation, and the expulsion of degradative products of the fibrils at 48 h, EGCG@SeNPs only started disaggregation of fibrils at 48 h. CD spectroscopy was applied to study the secondary structure of fibrils under the presence of both SeNPs (conditions shown in Table 3). While Aβ monomer exhibited a random-coil conformation spectrum, with a negative peak at 195 nm, Aβ fibrils showed a B-sheet structure, with a negative peak at 218 nm. In presence of Tet-1-EGCG@SeNPs at different incubation times, β-sheet structure was transformed into a random-coil conformation, indicative of the presence of amorphous aggregates. The higher presence of H-bond sites in Tet-1 peptide, may allow the higher interaction with Aβ fibrils.

Selenium nanoparticles stabilized with chitosan (Ch-SeNPs) had also demonstrated an elevated ability in inhibition and disaggregation of metal-induced $A\beta_{42}$ aggregation [71]. Aggregation and fibril morphology were studied by TEM with negative staining and ImageJ software treatment of micrographs (conditions shown in Table 3). Essential metal ions such as Fe(II), Cu(II) and Zn(II) favored amyloid aggregation, however co-incubation of $A\beta_{42}$ with Ch-SeNPs prevented fibrils accumulation at 48 h. Additionally, these NPs were able to disaggregate pre-formed fibrils due to Fe(II) effect at 24 h, demonstrating their enormous potential in AD treatment. Continuing with Ch-SeNPs, their effect over enantiomerically-induced amyloid aggregation had been also studied [72]. Due to the deleterious effect of D-enantiomers of amino acids in AD, as the chiral environment affects Aβ, the need for chiral drugs is of increasing interest. As it is widely known, chitosan possesses chirality, which may be useful to inhibit enantiomerically-induced $A\beta_{42}$ aggregation. In this work, authors demonstrated the preference of D-amino acids over L-amino acids, being the former the non-naturally present in human organisms, in increasing amyloid aggregation and fibrils width. However, Ch-SeNPs were shown to interact with D-enantiomers, while not with L-enantiomers, by UV–Vis and fluorescence spectroscopy, and in some cases, stoichiometry could be elucidated. Therefore, they were able to inhibit the enantiomerically-induced aggregation of $A\beta_{42}$ (conditions shown in Table 3). Taking these results into account, Ch-SeNPs are a promising drug against AD and should be further investigated.

Chondroitin sulphate (CS) possess diverse biological properties, such as antioxidant, anti-inflammation and neuroprotective. Therefore, selenium-chondroitin sulphate nanoparticles (CS@SeNPs) have been *in vitro* studied in AD field [34]. Regarding $A\beta_{42}$ aggregation kinetics, ThT fluorescence and Congo red assays were employed (conditions shown in Table 3). In ThT assay, while $A\beta_{42}$ alone presented a maximum of (103 ± 4) a.u., in presence of 50 μg mL^{-1} CS@SeNPs intensity decreased to (81 ± 2) a.u. By Congo red assay, $A\beta_{42}$ alone had a maximum of 0.24 a.u., while in presence of CS@SeNPs at 25 μg mL^{-1} absorbance decreased to 0.13, and at 50 μg mL^{-1} decreased to 0.8. Employing CD, monomeric $A\beta_{42}$ presented a random-coil structure, while $A\beta_{42}$ incubated for 3 days changed secondary structure towards a β-sheet rich form with a negative peak at 216 nm. In presence of 25 μg mL^{-1} CS@SeNPs secondary structure presented the same pattern with a decrease in the band at 216 nm. Nevertheless, at 50 μg mL^{-1} the structure was similar to monomeric $A\beta_{42}$, showing the ability of these NPs to inhibit the transition to β-sheet in $A\beta_{42}$, and therefore preventing amyloid plaques formation. Employing 1-anilino-8-naphthalene sulphate (ANS), authors could quantify the hydrophobicity of Aβ fibrils (conditions shown in Table 3). ANS is a commonly employed extrinsic fluorescent protein probe that exhibits distinctive fluorescence emission when it binds to hydrophobic regions located on the protein surface. Its application is widespread in assessing the likelihood of hydrophobic regions within a protein. $A\beta_{42}$ alone showed a fluorescence intensity of (410 ± 7) a.u., while in presence of 25 and 50 μg mL^{-1} CS@SeNPs, intensity was reduced to (370 ± 7) and (358 ± 9) a.u., respectively. In order to study fibrils morphology, TEM assay was employed as described in Table 3. $A\beta_{42}$ incubated for 3 days formed long branched fibrils, while in presence of CS@SeNPs many amorphous oligomers and short fibrils were observed. This decrease in fibrils length was dose-dependent, obtaining the most promising results at 50 μg mL^{-1} CS@SeNPs. Results were consistent with CD analysis, were the highest concentration of CS@SeNPs inhibited β-sheet formation.

Biogenic SeNPs from *Lactobacillus casei* have been also tested against $A\beta_{25\text{-}35}$ toxicity [80]. For this purpose, Aβ aggregation was monitored by fluorescence spectroscopy employing ThT (conditions shown in Table 3). This assay demonstrated that the fragment 25–35 of Aβ reached a maximum of aggregation at 7 days, when incubated at 37 °C, and SeNPs were able to reduce fluorescence maximum, therefore inhibiting amyloid aggregation.

Additionally, effect of selenium-doped carbon quantum dots (SeCQDs) against $A\beta_{40}$ has been tested *in vitro* [65]. Employing fluorescence spectroscopy and ThT assay, $A\beta_{40}$ effect increased ThT fluorescence reaching a maximum of intensity at 7 days (conditions shown in Table 3). However, the presence of SeCQDs (5 and 50 μg mL^{-1}) inhibited the aggregation process, slowing the kinetic reaction and reducing the maximum intensity, in a dose-dependent manner. By employing circular dichroism (CD), SeCQDs were able to inhibit the transition to β-sheet conformation of $A\beta_{40}$ (Table 3). In addition, by TEM analysis, SeCQDs inhibited Aβ fibrillization process, stopping the assembling into mature fibrils. To further understanding the binding to $A\beta_{40}$, nuclear magnetic resonance (NMR) spectroscopy was applied (Table 3). SeCQDs broadened His and Tyr10 lines of $A\beta_{40}$ and shifted Lys and Glu resonances to high-field, confirming the direct interaction of SeCQDs with Aβ residues or the induction of structural changes in this protein. This could be explained by the possible electrostatic interactions between the negative charged surface of SeCQDs, in contrast with to cationic cluster HHQK of the amyloid protein. This interaction could be the reason of the inhibition activity against amyloid aggregation.

On the other hand, chiral penicillamine-capped selenium nanoparticles (L-/D-Pen@SeNPs) have demonstrated excellent anti-amyloidogenic properties [76]. To study their inhibition of $A\beta_{40}$-induced aggregation, fluorescence spectroscopy using ThT assay was applied (conditions shown in Table 3). While Zn(II) increased the aggregation rate of fibrillation (maximum of fluorescence at 30 min), addition of L-/D-Pen@SeNPs delayed the fibrillation process, increasing the time to reach the plateau (40–60 min). While L-Pen@SeNPs only decreased the maximum intensity by 30 %, D-Pen@SeNPs inhibited it by 42 %. As observed by CD, $A\beta_{40}$ incubated during 48 h changed its structure from random coil to β-sheet, with a negative peak at 215 nm. The presence of Zn(II) in the incubation process increased the intensity of this peak, confirming the formation of more β-sheet structures. While both enantiomers successfully reduced the intensity of the band at 215 nm, D-Pen@SeNPs demonstrated a greater ability in the inhibition of β-sheet structure. TEM analysis showed various amorphous aggregates with heterogeneous oligomers when $A\beta_{40}$ was incubated with Zn(II) (conditions shown in Table 3). While D-Pen@SeNPs decreased the size of the amorphous aggregates, L-Pen@SeNPs had almost no effect.

In conclusion, the techniques and methods employed in this field have provided valuable insights into $A\beta_{42}$ aggregation, and the potential of SeNPs in inhibiting amyloid formation and protecting against AD-related toxicity. Molecular fluorescence using ThT has proven to be an accurate technique for quantifying amyloid aggregation and evaluating the kinetics of the aggregation process. TEM has allowed the visualization of $A\beta_{42}$ fibrils and the estimation of their length and width, providing crucial data on the morphology of the aggregates. RLS has demonstrated its high sensitivity in detecting the binding of $A\beta_{42}$ fibrils to NPs, offering valuable information about nanoparticle-protein interactions. The surface modification of SeNPs with polyphenols such as resveratrol, CGA, and Tet-1-EGCG has shown promising results in inhibiting amyloid aggregation and interfering with the binding of metal ions to $A\beta_{42}$ fibrils. The biogenic SeNPs derived from *Lactobacillus casei* and SeCQDs have also demonstrated inhibitory effects on Aβ aggregation. Chiral L-/D-Pen@SeNPs have exhibited excellent anti-amyloidogenic properties, with D-Pen@SeNPs showing a greater ability to inhibit β-sheet structure formation. Overall, these findings support the potential of SeNPs as therapeutic agents for the treatment of AD, providing new avenues for future research and drug development in the field of neurodegenerative disorders.

3.2. Bioanalytical assessment of selenium nanoparticles neuroprotection in cell lines: unravelling mechanisms and efficacy

This section focuses on the *in vitro* evaluation of the neuroprotective properties of SeNPs using different cell lines relevant to AD research. By employing bioanalytical techniques several aspects have been explored,

including the cytotoxicity of SeNPs, their intracellular effects, accumulation within cells, and antioxidant properties.

The choice of appropriate cell lines is crucial for studying AD-related mechanisms and evaluating potential therapeutic interventions. Commonly used cell lines such as PC12, SH-SY5Y, N2a, and SN56 offer valuable models for investigating AD pathology and assessing the efficacy of neuroprotective agents. By employing these cell lines, researchers have gain insights into the cellular responses to SeNPs and their impact on AD-related processes.

Bioanalytical techniques play a fundamental role in elucidating the mechanisms underlying the neuroprotective effects of SeNPs. These techniques allow the assessment of the cytotoxicity of SeNPs and their ability to reduce AD-induced cytotoxicity in cell lines. Moreover, they provide valuable information about the intracellular effects of SeNPs, including their accumulation patterns and potential interactions with cellular components. Additionally, the antioxidant properties of SeNPs can be evaluated using these techniques, shedding light on their potential to mitigate oxidative stress, a key factor in AD pathogenesis.

The findings obtained from *in vitro* studies employing cell lines contribute to our understanding of the therapeutic potential of SeNPs in AD. By elucidating the mechanisms underlying neuroprotective effects of SeNPs and their interactions with cellular components, these studies provide a foundation for further research and development of SeNPs as potential therapeutic interventions for AD.

3.2.1. Overview of main cell lines undergoing in AD research

Several cell lines have emerged as valuable models to study AD-related processes and explore the neuroprotective effects of various compounds. Here, an overview of the primary cell lines employed in AD research (Fig. 3) and highlights their significance in advancing our understanding of the disease is provided.

Rat pheochromocytoma (PC12) cell line, originally derived from a rat adrenal medullary tumor, has been extensively utilized in AD studies due to its ability to differentiate into a neuronal phenotype [98]. This cell line exhibits characteristics of sympathetic neurons and has proven valuable for investigating cellular processes involved in AD pathogenesis, such as neurotoxicity, oxidative stress, and neuroinflammation. PC12 cells have been instrumental in elucidating the molecular mechanisms underlying Aβ-induced neurotoxicity and the evaluation of potential neuroprotective agents. Several studies have reported their use for *in vitro* assessment of SeNPs neuroprotection [55,62,65,74,76,80].

Additionally, adipose mesenchymal stem cells (AMSCs) have gained recognition as a valuable cell line in AD research [99]. AMSCs, derived from adipose tissue, possess the ability to differentiate into multiple cell types, including neuronal-like cells. These cells offer a unique advantage in AD research by providing a model that closely mimics the physiological environment of the brain. AMSCs have been utilized to study various aspects of AD, including Aβ metabolism, neuroinflammation, and neurogenesis. Their regenerative properties and potential for neuronal differentiation make AMSCs a promising tool for investigating novel therapeutic approaches and regenerative strategies in AD. The

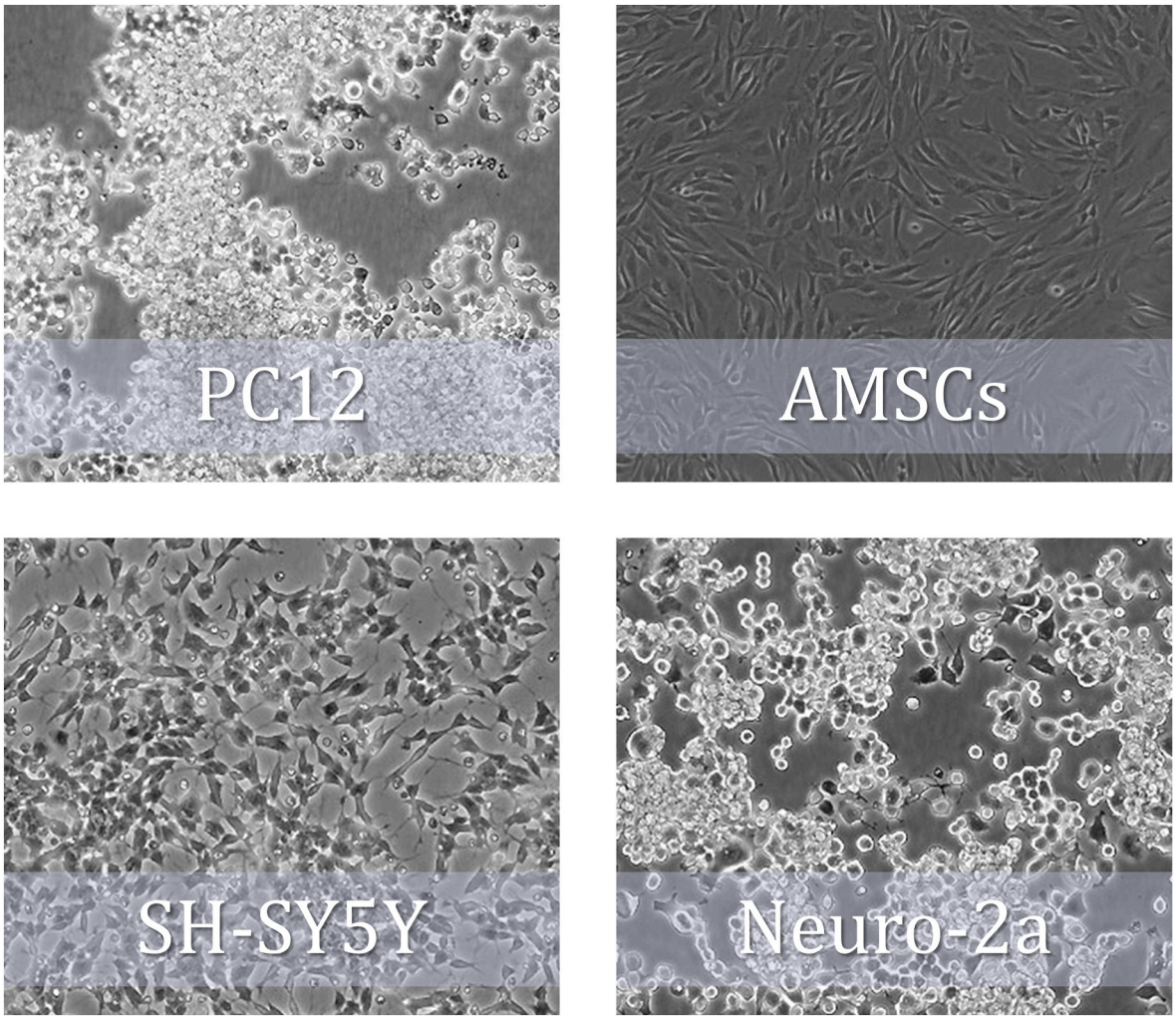

Fig. 3. Main cell lines employed in AD research (ATCC).

inclusion of AMSCs as a cell line in AD research broadens the scope of investigation and adds another dimension to our understanding of the disease processes involved.

Another widely used cell line in AD research is SH-SY5Y, a human neuroblastoma cell line [100]. SH-SY5Y cells possess dopaminergic neuronal characteristics and can be differentiated into mature neurons, making them suitable for studying AD-related processes. This cell line has been employed to investigate Aβ aggregation, tau phosphorylation, mitochondrial dysfunction, and neuronal cell death [34]. The SH-SY5Y cell line offers a valuable model to explore the cellular mechanisms involved in AD pathology and assess the therapeutic potential of various compounds.

Neuro-2a cells, derived from a mouse neuroblastoma, have also played a significant role in AD research [73]. Neuro-2a cells exhibit neuronal characteristics and have been utilized to study Aβ metabolism, cellular signaling pathways, and neuronal differentiation. These cells provide a platform to investigate the impact of various interventions on Aβ production, clearance, and neurotoxicity, contributing to our understanding of AD pathogenesis.

In summary, the selection of appropriate cell lines is crucial for advancing our knowledge of AD pathogenesis and evaluating potential therapeutic interventions. Each cell line provides a unique perspective, allowing to explore various aspects of AD pathology and assess the efficacy of potential neuroprotective agents. The utilization of these cell lines has contributed to the progress in understanding AD and provides a solid foundation for future studies aimed at developing effective treatments for this debilitating disorder.

3.2.2. *Main bioanalytical techniques employed in AD cellular studies*

In this section, the main bioanalytical techniques used in cellular studies related to AD will be introduced. These techniques can be categorized into three subgroups: cytotoxicity assays, accumulation and intracellular effect analysis, and oxidative stress assessment (Fig. 4).

Cytotoxicity assays play a crucial role in evaluating the toxic effects of compounds on cells. Two commonly employed methods within this category are UV–Vis spectroscopy, applied to MTT and CCK-8 assays, and flow cytometry utilizing propidium iodide (PI) staining. UV–Vis spectroscopy has been extensively used in MTT and CCK-8 assays to assess cell viability. These colorimetric assays rely on the conversion of tetrazolium salts into formazan crystals by mitochondrial enzymes in viable cells. The resulting absorbance is measured using UV–Vis spectroscopy, providing quantitative information about cell viability [70]. On the other side, flow cytometry employing with PI staining, allows for the assessment of cell death. PI, a DNA intercalating agent, is impermeable to live cells but enters and stains the DNA of dead or dying cells. By analyzing the fluorescence emitted by propidium iodide-stained cells using flow cytometry, it is possible to quantify the extent of cytotoxicity in a cell population [73].

Understanding the accumulation and intracellular effects of molecules within cells is crucial for studying the mechanisms underlying AD. Several techniques commonly employed in this regard are microscopy techniques, fluorescence spectroscopy, and ICP techniques. Microscopy techniques, such as TEM, provide high-resolution imaging of cellular structures. In this context, TEM allows to examine the accumulation of SeNPs by cell population and observe their impact on cellular morphology [73]. Fluorescence spectroscopy techniques, ThT and 4′, 6-diamidino-2-phenylindole (DAPI) or Hoechst 33342 staining, offer valuable insights into the intracellular localization of specific molecules. ThT is a fluorescent dye that binds to amyloid fibrils, enabling the detection and quantification of their accumulation. DAPI and Hoechst 33342 are DNA-intercalating dyes used to visualize the nuclei of cells, aiding in the analysis of nuclear alterations [34]. Inductively coupled plasma techniques, such as inductively coupled plasma atomic emission spectroscopy (ICP-AES) and inductively coupled plasma mass spectrometry (ICP-MS), provide quantitative measurements of elemental composition in cellular samples. These techniques have been employed to investigate the accumulation of selenium in cell populations [74].

Oxidative stress is a critical factor in AD progression, and its assessment within cellular studies is of immense importance. Several techniques commonly used to evaluate oxidative stress include fluorescence microscopy, flow cytometry, and fluorescence spectroscopy, all employing the fluorescent probe 2′,7′-dichlorofluorescin diacetate (DCFH-DA). Fluorescence microscopy enables the visualization and quantification of ROS generation within cells. By measuring the fluorescence intensity of the oxidized product, it is possible to assess the extent of oxidative stress in specific cellular compartments [80]. Flow cytometry and fluorescence spectroscopy allow for the quantitative analysis of ROS levels in a cell population. By monitoring the

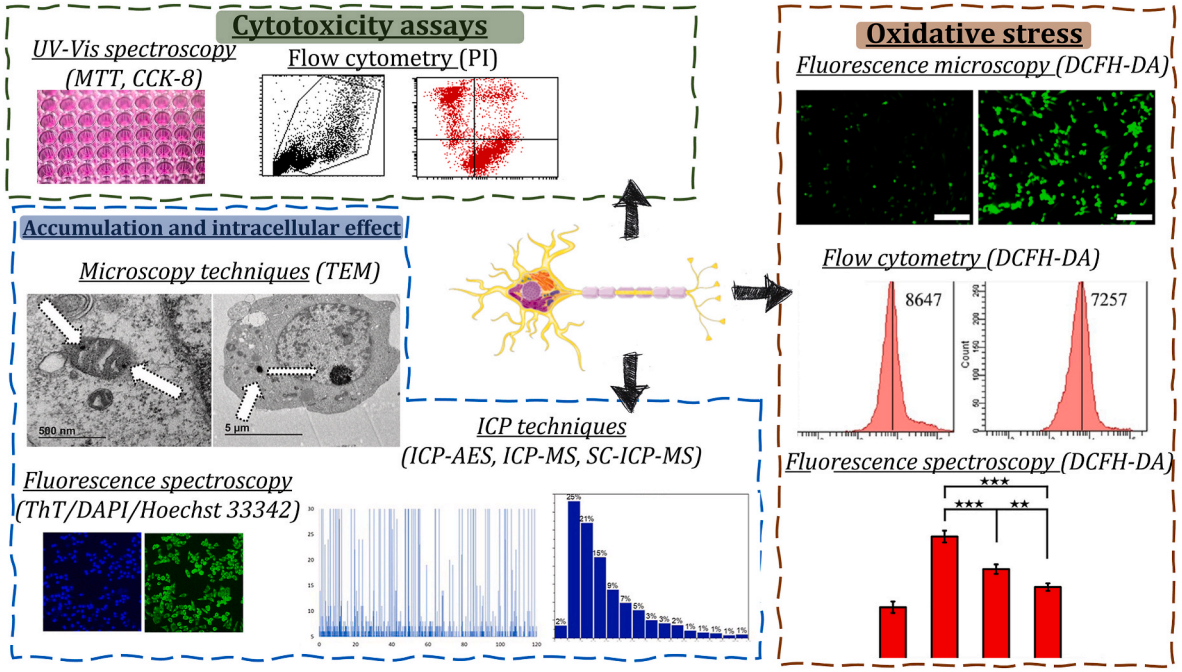

Fig. 4. Main bioanalytical techniques for *in vitro* neuroprotective studies in cell lines.

fluorescence signal, the overall response to oxidative stress can be assessed in a high-throughput manner [55].

In summary, the utilization of bioanalytical techniques within cellular studies in the field of AD is vital for understanding disease mechanisms and identifying potential therapeutic targets. Cytotoxicity assays, accumulation and intracellular effect analysis, and oxidative stress assessment techniques contribute significantly to our knowledge of the cellular processes underlying AD pathology (Table 4).

3.2.3. *Cytotoxicity of selenium nanoparticles and reduction of AD-induced cytotoxicity in cell lines*

The assessment of cytotoxicity is crucial when evaluating the potential applications of SeNPs. Various techniques and methods are employed to determine cell viability and detect cellular changes associated with cytotoxicity. This section explores the utilization of different techniques such as the 3-(4,5- dimethylthiazol-2-yl)-2,5-diphenyltetrazole bromide (MTT) colorimetric assay, flow cytometry with fluorochromes, terminal deoxynucleotidyl transferase dUTP nick end labelling (TUNEL)- DAPI co-staining, and lactate dehydrogenase (LHD) analysis to evaluate the cytotoxicity of SeNPs.

MTT assay is a widely used colorimetric method, for assessing cell viability and proliferation, which measures the metabolic activity of cells [101]. The MTT assay is commonly used for evaluating the cytotoxicity of compounds, NPs, or drugs, as well as assessing the effects of various treatments or conditions on cell viability. It is a simple, rapid, and cost-effective assay that provides quantitative information about cell viability and can be adapted to high-throughput screening.

Flow cytometry is a powerful analytical technique used to analyze and quantify characteristics of individual cells or particles in a heterogeneous population [102]. It utilizes the principles of fluid dynamics and laser-based detection. In a flow cytometry assay, cells are labelled with fluorescently labelled antibodies or dyes, mainly propidium iodide (PI), that bind to specific molecules or cellular components of interest. By this way, flow cytometry can provide information about cell viability, proliferation, differentiation, apoptosis, and the expression of cell surface markers. It enables the identification and characterization of different cell populations within a sample and allows for the study of complex cellular processes at the single-cell level. Flow cytometry is widely used in various fields, including immunology, cancer research, stem cell biology, and microbiology, due to its high throughput, sensitivity, and versatility in analyzing multiple parameters simultaneously.

In TUNEL-DAPI assay, DNA strand breaks in apoptotic cells are labelled by incorporating fluorescently labelled nucleotides at the free 3′-OH ends of fragmented DNA [62]. By combining TUNEL labelling and DAPI staining, the TUNEL-DAPI assay allows for the visualization and quantification of apoptotic cells with fragmented DNA. Apoptotic cells typically exhibit bright fluorescent labelling in their nuclei due to the presence of DNA breaks. This assay provides valuable information on the initial stages of DNA fragmentation in apoptotic cells and can be used in conjunction with other techniques to study cell death processes, evaluate the efficacy of potential therapeutic interventions, and assess the cytotoxicity of various agents or NPs.

LHD assay is a commonly used method to assess cell membrane damage and cytotoxicity [103]. LHD, or lactate dehydrogenase, is an enzyme present in the cytoplasm of cells. By quantifying the amount of LHD released, the LHD assay provides a quantitative measure of cell membrane integrity and can be used to evaluate the cytotoxic effects of various compounds, NPs, or treatments. It is a valuable tool in assessing cell viability, cytotoxicity, and the protective effects of agents against membrane damage.

Briefly, the assessment of cytotoxicity is essential in understanding the potential applications of SeNPs. Techniques such as the MTT assay, flow cytometry with fluorochromes, TUNEL-DAPI co-staining, and LHD analysis provide valuable insights into cell viability, apoptosis, DNA

Table 4
Comprehensive bioanalytical approaches for the assessment of bioanalytical parameters in AD cell populations regarding SeNPs effect.

Bioanalytical parameter	Method	Technique	Experimental conditions					Reference
Cytotoxicity	MTT	UV–Vis spectroscopy	***Incubation time (days)***	***MTT (mg L^{-1})***		***Absorption wavelength (nm)***	***Aβ (μM)***	
			2	*Not specified*		*Not specified*	35	[55]
			1	*Not specified*		570	10	[65]
			1, 2, 3	*Not specified*		*Not specified*	–	[70]
			3	*Not specified*		*Not specified*	35	[62]
			2	*Not specified*		*Not specified*	20	[74]
			2	0.5		570	–	[73]
	CCK-8		***Incubation time (days)***	***CCK-8***		***Absorption wavelength (nm)***	***Aβ (μM)***	
			2	*Not specified*		450	25	[80]
			1	*Not specified*		450	20	[34]
	PI	Flow cytometry	***Incubation time (days)***	***IP (μg mL^{-1})***		***Excitation/emission wavelength (nm)***		
			2	2		535/617		[73]
Oxidative stress	DCFH-DA	Fluorescence spectroscopy	***Medium (pH)***	***Incubation time (days)***	***DCFH-DA (mM)***	***Under darkness (min)***	***Excitation/emission wavelength (nm)***	***Aβ (μM)***	
			50 mM PBS (7.4)	5	0.1	Not specified	488/525	35	[55]
			10 mM Tris, 150 mM NaCl (7.4)	7	0.02	60	488/525	100	[65]
			PBS	6 (h)	0.005	30	488/525	10	[34]
		Flow cytometry		2	10	Not specified	488/525	35	[55]
			PBS	3	10	30	488/525	35	[62]
			Not specified	1	0.005	30	488/530	20	[74]
		Fluorescence microscopy	*Not specified*	2	0.01	20		25	[80]
			PBS	3	10	30	488/525	35	[62]
Intracellular Aβ-fibrillation	ThT/DAPI	Fluorescence microscopy	***Medium (pH)***	***Incubation time (days)***	***ThT (%)***	***DAPI (μg mL^{-1})***	***Excitation/emission wavelength (nm)***	***Aβ (μM)***	
			10 mM PBS (7.4)	2	0.05	1	Not specified/480	20	[74]
			Not specified	2	0.05	1	440/488	10	[76]
	ThT/ Hoechst 33342		***Medium (pH)***	***Incubation time (days)***	***ThT (%)***	***Hoechst 33342***	***Excitation/emission wavelength (nm)***	***Aβ (μM)***	
			PBS	2	Not specified	Not specified	Not specified	10	[34]

fragmentation, and membrane integrity. These methods have been employed in numerous studies to evaluate the cytotoxicity of SeNPs and assess their potential protective effects against different cytotoxic agents.

Res@SeNPs have been tested *in vitro* with PC12 cells against Cu(II)-induced $A\beta_{42}$ cytotoxicity during 48 h by MTT assay (experimental conditions shown in Table 4) [55]. While $A\beta_{42}$ produced a cell viability of 46 %, $A\beta_{42}$-Cu(II) decreased viability to 32 %. However, Res@SeNPs increased cell viability to 93 %, protecting PC12 cells from $A\beta_{42}$-Cu(II) cytotoxicity. Additionally, extracellular lactate dehydrogenase (LHD) levels, as an indicator of cell membrane damage, were analyzed by using a commercial kit. While $A\beta_{42}$ and $A\beta_{42}$-Cu(II), increased cell membrane damage (142 % and 213 %, respectively), Res@SeNPs were able to prevent membrane integrity, achieving normal LHD levels. $A\beta_{42}$ and $A\beta_{42}$-Cu(II) also demonstrated to induce early apoptotic death in PC12 cells, by using TUNEL-DAPI co-staining. However, in presence of Res@SeNPs, DNA fragmentation decreased significatively, suggesting that this SeNPs could mitigate $A\beta_{42}$-Cu(II) apoptotic activity in PC12 cells.

CGA@SeNPs demonstrated to reduce cytotoxicity of $A\beta_{40}$ against PC12 cells by MTT method (conditions shown in Table 4) [62]. While 35 μM $A\beta_{40}$ produced a 47 % decrease in cell viability, co-treatment with 60 μg mL^{-1} CGA@SeNPs only reduced cell viability by 5 %, protecting cells against $A\beta_{40}$ toxicity. Regarding membrane integrity, $A\beta_{40}$ increased 142 % LDH levels, while in presence of CGA@SeNPs LDH levels were statistically similar to control. Therefore, CGA@SeNPs could prevent membrane integrity against $A\beta_{40}$ effect. By using TUNEL-DAPI co-staining and fluorescence microscopy, CGA@SeNPs were able to counteract cell apoptosis induced by $A\beta_{40}$, reducing fluorescent green intensity of apoptotic nuclei, and protecting neurons from apoptotic death.

EGCG@SeNPs and Tet-1-EGCG@SeNPs cytotoxicity was tested against PC12 cells by MTT assay (conditions shown in Table 4) [74]. While Aβ at 20 μM decreased cell viability to 56 %, the presence of EGCG@SeNPs and Tet-1-EGCG@SeNPs at 10 μg mL^{-1} increased this percentage to 75 % and 88 %, respectively. TUNEL-DAPI co-staining assay was applied to test protection against DNA fragmentation induced by Aβ fibrils, observed by a fluorescence microscope. While these fibrils provoked an increase in DNA fragmentation and nuclear condensation, both types of SeNPs reduced these effects, demonstrating their ability to transform Aβ fibrils into other structures that resulted in less induction of DNA fragmentation.

Cytotoxicity of selenium nanoparticles stabilized with chitosan (Ch-SeNPs) has been evaluated *in vitro* against adipose mesenchymal stem cells (AMSC) employing MTT method (conditions shown in Table 4) [70]. Ch-SeNPs (0.01, 0.1, 1 and 10 μg mL^{-1}) were able to increase cell proliferation at 24 (20, 20, 22.5, and 25 %, respectively), 48 (20, 15, 15, and 15 %, respectively) and 72 h (20, 15, 10 and 10 %, respectively), in comparison with the control group. In addition, Ch-SeNPs at 10 μg mL^{-1} were able to decrease LDH levels after 24 (40 %), 48 (20 %) and 72 h (43 %) treatment, which indicates their ability to protect cell membrane damage.

Additionally, Ch-SeNPs have been *in vitro* evaluated employing mouse (Neuro-2a) and human (SH-SY5Y) neuroblastoma cell lines [73]. Regarding cytotoxicity assays, two methods were employed: MTT and flow cytometry (conditions shown in Table 4). For this purpose, Ch-SeNPs at various concentrations (50–1000 μM) were evaluated at 48 h of exposure. Results showed that Neuro-2a cells were more sensitive than SH-SY5Y to Ch-SeNPs toxicity. Moreover, MTT method and flow cytometry assay offered similar cytotoxicity values for SH-SY5Y cells, while differences between methods were found in Neuro-2a cells. This distinction can be attributed to the different metabolic activity of mammalian cells in relation to mitochondrial dehydrogenases. However, Ch-SeNPs at 50 μM had no significant effect on cell viability in any cell line. Lethal concentration for 50 % of cell population values for Neuro-2a were ranged between (250 ± 30) and (330 ± 20) μM, while for SH-SY5Y were (350 ± 10) and (430 ± 10) μM, for MTT and flow cytometry methods, respectively.

Reduction of $A\beta_{42}$-induced cytotoxicity in SH-SY5Y cell line by CS@SeNPs employing CCK-8 assay as described in Table 4 [34]. While 20 μM $A\beta_{42}$ reduced cell viability to (70 ± 2)% at 24 h, co-incubation with 25 and 50 μg mL^{-1} increased cell viability to (80 ± 6)% and (103 ± 9)%, respectively. Therefore, CS@SeNPs could mitigate $A\beta_{42}$ cytotoxicity in a dose-dependent manner.

Biogenic SeNPs from *Lactobacillus casei* demonstrated to reduce the cytotoxicity of $A\beta_{25\text{-}35}$ in PC12 cells [80]. $A\beta_{25\text{-}35}$ toxicity was tested at two different concentrations (25 and 50 μM) at two different incubation times (24 and 48 h). Since Aβ toxicity was statistically similar for both concentrations at 48 h, authors chose 25 μM (24.42 % of cytotoxicity) to perform the following experiments. Biogenic SeNPs, from 0 to 64 μg mL^{-1}, demonstrated no cytotoxicity in PC12 cells, while pre-treatment of cells during 12 h with SeNPs (2, 4 and 8 μg mL^{-1}) mitigate $A\beta_{25\text{-}35}$ toxicity, in a dose-dependent manner. Regarding membrane integrity, LDH levels were measured under the effect of 25 μM of $A\beta_{25\text{-}35}$ during 48 h, observing higher LDH release than cells pre-treated with 8 μg mL^{-1} of SeNPs. Therefore, biogenic SeNPs could protect membrane integrity from Aβ effect. $A\beta_{25\text{-}35}$ increased AChE activity by 10 %, while pre-treatment with 8 μg mL^{-1} SeNPs reduced its activity to similar levels than control. Moreover, SeNPs were able to inhibit $A\beta_{25\text{-}35}$-induced apoptosis and necrosis, confirmed by fluorescence of Hoechst33342 nuclear dying agent and Annexin V-FITC/PI staining. The inflammatory response in PC12 cells induced by $A\beta_{25\text{-}35}$ was measured by the monitorization of the increase of pro-inflammatory (IL-1β and IL-18) and decrease of anti-inflammatory (IL-4 and IL-10), cytokine levels. Pre-treatment with SeNPs decreased pro-inflammatory cytokines while increased anti-inflammatory ones, counteracting $A\beta_{25\text{-}35}$ effect.

Ability of SeCQDs against $A\beta_{40}$-induced cytotoxicity in PC12 cell line had also been investigated, employing MTT method (conditions shown in Table 4) [65]. $A\beta_{40}$ decreased cell viability to 54 % at 24 h, while pre-treatment with SeCQDs (0.5 and 5 μg mL^{-1}) prevented this cytotoxicity in a dose-dependent manner (80 % and 90 %, respectively).

In conclusion, the studies discussed in this section provide evidence for the potential of SeNPs in mitigating cytotoxicity and protecting cells against various toxic agents. The techniques and methods employed, such as the MTT assay, flow cytometry with fluorochromes, TUNEL-DAPI co-staining, and LHD analysis, have been instrumental in evaluating the cytotoxic effects of SeNPs and assessing their protective properties. Further research is warranted to explore the underlying mechanisms and optimize the use of SeNPs in biomedical applications.

3.2.4. Accumulation and intracellular effect of SeNPs in cell lines

The accumulation and intracellular effects of SeNPs in cell lines have been a subject of investigation in the field of AD. Various techniques and methods have been employed to study the internalization, distribution, and impact of SeNPs within different cell types. This section focuses on the utilization of fluorescence spectroscopy, microscopy, and ICP analysis, among others, to investigate the behavior of SeNPs in cell lines.

Biogenic SeNPs from *Lactobacillus casei* were able to internalize in PC12 cells, as observed by TEM [80]. Se signal was observed by EDX, confirming the presence of this NPs in cytoplasm of PC12 cells by endocytosis. However, no evidence of nuclear internalization was shown in this research.

Fluorescence microscopy is a technique which allow to visualize intracellular Aβ aggregates, by the proper staining of fibrils with ThT and DAPI [76]. By this method, L-/D-Pen@SeNPs have been tested to counteract $A\beta_{40}$ intracellular aggregation (conditions shown in Table 4). While D-Pen@SeNPs successfully achieved to reduce ThT fluorescence induced by Zn(II), L-Pen@SeNPs did not show anti-amyloidogenic activity. Inhibition of intracellular $A\beta_{40}$ aggregation due to D-Pen@SeNPs could be related to their enhanced cellular uptake by PC12 cells.

EGCG@SeNPs and Tet-1-EGCG@SeNPs cellular uptake has been quantified by ICP-AES in PC12 cells [74]. For this purpose, 10^7 cells

were incubated in presence of both types of SeNPs (5 and 10 μg mL^{-1}) during 12 h, being washed afterwards. An acid digestion employing HNO_3 and H_2O_2 at 180 °C during 90 min was performed, and samples were analyzed by ICP-AES. While EGCG@SeNPs at 10 μg mL^{-1} increased Se content from 0.09 μg to 1.4 μg, Tet-1-EGCG@SeNPs at 5 and 10 μg mL^{-1} increased Se to 2.8 and 5.6 μg respectively, being therefore the most accumulated by this cell line. Intracellular Aβ aggregation was detected by ThT and DAPI staining (conditions shown in Table 4). While EGCG@SeNPs at 10 μg mL^{-1} slightly reduced ThT fluorescence intensity, Tet-1-EGCG@SeNPs completely inhibited ThT signal, indicative of the enormous potential of the latter to inhibit intracellular Aβ fibrillation inside PC12 cells. The higher cellular uptake of this type of SeNPs may be related to their ability to inhibit amyloid aggregation.

The internalization pathway of Ch-SeNPs in SH-SY5Y cells has been studied by TEM, pre-fixed with paraformaldehyde/glutaraldehyde and post-fixed with osmium tetroxide [73]. These NPs were observed in three distinct stages of internalization (early, intermediate and advanced), as can be seen in Fig. 5. Since they were able to inhibit *in vitro* amyloid aggregation, their adherence to the outside part of the cell membrane in early (Fig. 5b) and intermediate (Fig. 5c) stages could be indicative to their enormous potential in the disruption of extracellular amyloid plaques. Due to the well-known antioxidant properties of selenium, presence of Ch-SeNPs inside mitochondria in intermediate stages (Fig. 5d) could be strongly beneficial to reduce mitochondrial DNA oxidation observed in AD patients. Nevertheless, in intermediate and advanced (Fig. 5e) stages, the Ch-SeNPs were able to cross the nuclear membrane, hence their effect inside the nucleus and nucleoli should be further studied.

With the aim of deepening into the accumulation of Ch-SeNPs inside neuroblastoma cell lines, ICP-MS in single cell mode (SC-ICP-MS) was employed to Neuro-2a and SH-SY5Y cells exposed to Ch-SeNPs (10, 50 and 250 μM) during 48 h [73]. Once more, SH-SY5Y cells offered higher accumulation of selenium than Neuro-2a, while both of them were able to accumulate Ch-SeNPs at every concentration tested in a dose-dependent manner. For 10, 50 and 250 μM, Neuro-2a accumulated a maximum of 37.4, 63.9 and 89.5 fg Se $cell^{-1}$, respectively, while SH-SY5Y demonstrated a maximum accumulation of 54.1, 76.8 and 129.8 fg Se $cell^{-1}$, respectively. Due to the high variability of selenium accumulation by neuroblastoma cells, selective techniques such as SC-ICP-MS are often used to provide solid information of selenium distribution in cell populations.

CS@SeNPs ability to inhibit intracellular $A\beta_{42}$ fibrillation inside SH-SY5Y cells was evaluated by ThT/Hoechst 33342 fluorescence assay, as shown in Table 4 [34]. In presence of $A\beta_{42}$, several green spots were observed in SH-SY5Y cells, indicative of the formation of intracellular fibrils. However, in presence of 25 μg mL^{-1} CS@SeNPs green fluorescence significatively decreased, and at 50 μg mL^{-1} nearly all fluorescence disappeared. Additionally, CS@SeNPs were able to reduce $A\beta_{42}$-induced hyperphosphorylation of tau at Ser_{396} and Ser_{404}, being therefore promising anti-AD drugs.

These findings emphasize the potential of SeNPs as therapeutic agents for AD and provide a better understanding of their intracellular behavior. The combination of fluorescence spectroscopy, microscopy, TEM, and ICP analysis has proven valuable in investigating the accumulation and intracellular effects of SeNPs in cell lines, paving the way for further research in the field of AD treatment.

3.2.5. Antioxidant properties of SeNPs in cell lines

Oxidative stress has emerged as a crucial factor in the pathogenesis of AD. The disruption in the equilibrium of pro-oxidant/antioxidant homeostasis is a major mechanism underlying oxidative stress. In recent years, various techniques and methods have been employed to investigate the antioxidant properties of SeNPs to mitigate the oxidative stress associated with AD.

One notable technique used to assess the antioxidant activity of SeNPs is the DCFH-DA assay, which measures the intracellular levels of ROS. In this method, the DCFH-DA molecule is internalized by cells and converted to DCFH in the presence of ROS. DCFH is non-fluorescent, but when oxidized by ROS, it is converted to 2′,7′-dichlorofluorescein (DCF), a highly fluorescent molecule.

On the other hand, flow cytometry is a technique that enables quantitative measurement and analysis of the physical and chemical characteristics of individual cells. In the case of the DCFH-DA assay, flow cytometry is used to quantify the fluorescence intensity generated by DCF in cells treated with SeNPs.

In flow cytometry, treated cells are suspended in a fluid and injected into a continuous flow in a flow cytometer. As the cells pass through the laser, they are excited and emit fluorescence, which is detected by photomultipliers. The fluorescence intensity measured in each cell correlates with the amount of ROS present, providing information about the level of oxidative stress in the cells.

In summary, the DCFH-DA method relies on its conversion to DCF in the presence of intracellular ROS, and flow cytometry is used to quantitatively measure and analyze the fluorescence intensity generated by DCF in treated cells. This combination of techniques allows for the accurate evaluation of ROS levels and the antioxidant capacity of the studied compounds.

Res@SeNPs have demonstrated great *in vitro* antioxidant properties in PC12 cells by DCFH-DA assay (conditions shown in Table 4) [55]. While Cu(II) increased $A\beta_{42}$-induced H_2O_2 levels by 263 % in comparison to control, Res@SeNPs reduced oxidative stress by 135 % in comparison with metal-treated cells.

CGA@SeNPs *in vitro* antioxidant activity against $A\beta_{40}$-induced ROS was evaluated in PC12 cells by DCFH-DA assay (conditions shown in Table 4) [62]. 35 μM of $A\beta_{40}$ produced an increase of 50 % of ROS in comparison to control, while 60 μg mL^{-1} of CGA@SeNPs reduced ROS to similar levels than control.

Moving on to polyphenol-stabilized SeNPs, EGCG@SeNPs and Tet-1-EGCG@SeNPs antioxidant activity was tested in PC12 cells by DCFH-DA assay and flow cytometry (conditions shown in Table 4) [74]. Aβ fibrils at 20 μM increased ROS production, achieving an intensity of 8647 counts, while the presence of SeNPs at 10 μg mL^{-1} during 72 h reduced oxidative stress to 5647 counts (EGCG@SeNPs) and 3678 counts (Tet-1-EGCG@SeNPs), being therefore potent antioxidant SeNPs.

Antioxidant properties of CS@SeNPs employing SH-SY5Y cell line and DCFH-DA method were evaluated, following conditions in Table 4 [34]. While 10 μM $A\beta_{42}$ increased fluorescence intensity up to 140 %, in presence of 25 and 50 μg mL^{-1} CS@SeNPs fluorescence was reduced to 70 % and 75 % in comparison with control, respectively. Therefore, these NPs were able to reduce ROS formation in human neuroblastoma cell line in a dose-dependent manner.

Biogenic SeNPs from *Lactobacillus casei* mitigated $A\beta_{25\text{-}35}$-induced oxidative stress in PC12 cells, by the monitorization of intracellular ROS generation by DCFH-DA assay and fluorescence microscopy (conditions shown in Table 4) [80]. $A\beta_{25\text{-}35}$ ROS generation was confirmed by 48 h of incubation in PC12 cells, while pre-treatment with 8 μg mL^{-1} of biogenic SeNPs for 12 h significatively decreased intracellular ROS levels.

SeCQDs were able to reduce the intracellular generation of ROS in PC12 cells, as confirmed by the DCFH-DA assay (conditions shown in Table 4) [65]. While $A\beta_{40}$ increased up to 236 % ROS levels, pre-treatment with SeCQDs (0.5 and 5 μg mL^{-1}) decreased their levels (173 % and 139 %, respectively).

The studies discussed in this section have shed light on the antioxidant properties of SeNPs in the context of AD. The results obtained through various techniques and methods have demonstrated the potential of SeNPs in mitigating oxidative stress, a significant factor in the pathogenesis of this neurological disorder. These findings highlight the importance of SeNPs as promising candidates for the development of novel antioxidant therapies for AD. Further research and *in vivo* studies are necessary to fully explore the therapeutic potential of SeNPs and to

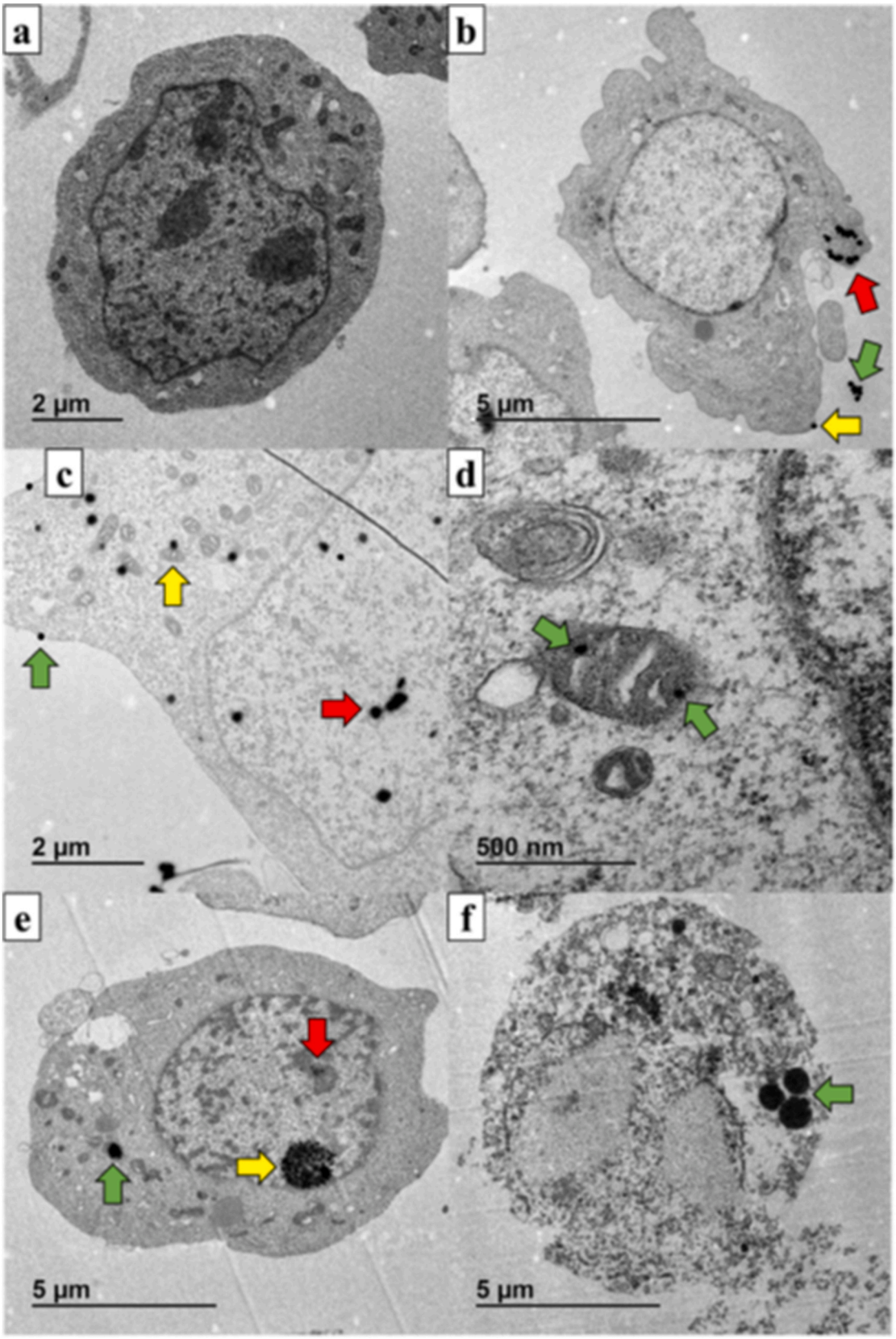

Fig. 5. Micrographs depicting the internalization of Ch-SeNPs (indicated by green, yellow, and red arrows) in SH-SY5Y cell line as observed through TEM. a) Control SH-SY5Y cell; b) SH-SY5Y cell in the early stage of Ch-SeNPs internalization; c) SH-SY5Y cell in the intermediate stage of Ch-SeNPs internalization; d) Localization of Ch-SeNPs inside mitochondria; e) SH-SY5Y cell in the advanced stage of Ch-SeNPs internalization; f) Deceased SH-SY5Y cell attributed to the effects of Ch-SeNPs. Figure obtained with permission of Vicente-Zurdo, D. et al. [73].

translate these findings into clinical applications. The use of SeNPs as antioxidants in AD treatment holds great promise and warrants continued investigation in the field of neurodegenerative diseases.

4. SeNPs and their role in AD treatment: *in vivo* studies

Traditionally, *in vivo* models have been deemed indispensable tools in preclinical research and for evaluating new pharmaceuticals. Rodent experiments remain crucial for AD studies, and various models utilizing genetic and non-genetic approaches are available in the market, facilitating the identification of key mechanisms involved in the disease's progression. Nevertheless, other animals, such as the *Caenorhabditis elegans* nematode, fruit fly, and zebrafish, have also been employed in AD research, benefitting from their complete genetic sequencing data. While some human genes linked to AD are present in these sequences, these models suffer from the drawback of differing significantly in anatomical and physiological characteristics from humans [104].

Studies involving SeNPs for *in vivo* assays have been conducted using both genetically modified mice and mice with induced disease symptoms (Table 5).

In AD research, mice have been utilized for testing novel drugs and investigating underlying biological mechanisms [105]. Given the occurrence of synaptic and cognitive impairments in the disease, *in vivo* investigations have focused on developing cognitive assays in mice, particularly examining memory and learning abilities associated with the hippocampus. Additionally, these studies delve into mechanisms

Table 5
SeNPs used in the diagnosis and therapy in mouse models of Alzheimer's disease.

Mouse model	Description	Nanoparticle	Studies in mouse	Ref.
APP/PS1	Transgenic	Penicillamine selenium nanoparticles L-/D-Pen@SeNPs	Cognitive ability (Morris water maze and Novel-object recognition test) Histological analysis	[76]
APP/PS1	Transgenic	Chlorogenic Acid-Selenium nanocluster Chlorogenic Acid-Selenium-peptide CGA@SeNCs TGN-CGA@SeNCs	Cognitive ability (Morris water maze, Novel-object recognition and open-field test) Glucose and Insulin tolerance Histological studies Gut microbiota analysis	[85]
APP/PS1	Transgenic	Dihydromyricetin-selenium Dihydromyricetin-selenium Chitosan Blood brain barrier peptide CS/DMY@SeNPs TGN-CS/DMY@SeNPs	Cognitive ability (Morris water maze test) Histological studies Gut microbiota analysis	[75]
APP/PS1	Transgenic	Mesoporous nano-selenium MSe-Res/Fc-β-CD/Bor	Cognitive ability (Morris water maze test) Immunohistochemistry and western blot Metabolic research of selenium	[64]
APP/PS1	Transgenic	Selenium-polydopamine nanozyme Se@PDA@Bor	Cognitive ability (Morris water maze test, nesting test) Immunohistochemistry Immunofluorescence	[83]
Male C57BL6/J	AD model induced $A\beta_{40}$ oligomers injected each side of hippocampus	Selenium-doped carbon quantum dots SeCQDs	Accumulation of NPs in brain by ICP-MS Cognitive ability (Morris water maze test) Immunohistochemistry of Aβ	[65]
Male C57BL/6	AD model induced D-gal 120 mg kg^{-1} day^{-1} Aluminum chloride 200 mg kg^{-1} day^{-1} for 60 days	Chondroitin sulphate nano-selenium CS@SeNPs	Cognitive ability (Morris water maze, Novel-object recognition and open-field test) Immunohistochemistry and wester blotting	[60]
Male ICR	AD model induced D-gal 120 mg kg^{-1} day^{-1} Aluminum chloride 50 mg kg^{-1} day^{-1} for 24 weeks	Resveratrol-loaded selenium chitosan nanoflowers Res@SeNPs@res–CS–NP	Cognitive ability (Morris water maze test) Blood glucose tolerance and insulin tolerance test Serum and liver biochemical and physiological index Intraperitoneal adipose tissue studies	[58]
Male ICR	AD model induced D-gal 60 mg kg^{-1} day^{-1} Aluminum chloride 35 mg kg^{-1} day^{-1} for 16 weeks	Resveratrol-Selenium -peptide nanocomposites TGN-Res@SeNPs	Cognitive ability (Morris water maze test) Histological studies Microbiome imbalances Liver and renal functions	[57]
Male Kunming	AD model induced $A\beta_{42}$ peptide	Selenium quantum dots nano selenium	Cognitive ability (Y-maze spontaneous alternating test, Novel-object recognition and open field test) Immunofluorescence	[66]
Male Wistar	AD model induced Aluminum chloride 100 mg kg^{-1} day^{-1} for 60 days	Resveratrol-Selenium RSV-SeNPs	Aβ-42 and Tau protein levels Neuroinflammatory markers Wester immunoblotting Histopathological studies	[56]
Male Wistar	AD model induced Streptozotocin 3 mg kg^{-1} day^{-1}	Selenium nanoparticles and mesenchyme stem cells AMSCs SeNPs	Cognitive ability (Novel-object recognition test) Histological studies Determination of brain derived neurotrophic factor (BDNF)	[61]
Male Wistar	AD model induced Streptozotocin 3 mg kg^{-1} day^{-1}	Chitosan-coated selenium nanoparticles and mesenchyme stem cells AMSCs SeNPs AMSCs Ch-SeNPs	Cognitive ability (Novel-object recognition test) Histological studies Determination of brain derived neurotrophic factor (BDNF)	[70]
Male Wistar	AD model induced Streptozotocin 3 mg kg^{-1} day^{-1} for 1 month	SeNPs	Passive avoidance learning Aβ deposition Oxidative stress and antioxidant capacity Histological studies	[68]
Male Wistar	AD model induced Streptozotocin 3 mg kg^{-1} day^{-1}	Polyvinyl alcohol selenium nanoparticles PVP-coated SeNPs	Cognitive ability (NOR and passive avoidance learning test) Hippocampal brain-derived neurotrophic factor (BDNF) Histological assessments Oxidative stress assessments	[69]

related to the formation of Aβ protein deposits, neuroinflammation processes, the role of the microbiota in AD's etiology, oxidative damage, autophagy, implications of the Tau protein, and vascular dysfunctions [104] (Fig. 6).

Assorted options exist for employing genetically modified mice to assess the therapeutic potential of different SeNPs. However, researchers have predominantly utilized double transgenic APP/PS1 mice [64,75,76,83,85] for these investigations. This particular model features 30 mutations in the transmembrane glycoprotein type I (APP) and 200 mutations in PS1. These mutations have been identified in families with early-onset AD, showing an overexpression of pathology related to the development of amyloid plaques, synaptic loss, cognitive deficits, and impaired synaptic plasticity [105].

Indeed, a significant concern associated with using genetically modified mice is the potential distortion of data in research studies. The pathogenesis and overexpression of related genes in these mice can lead to unintended effects on neuronal functions, which may not be directly linked to the Aβ protein or the pathology of AD. Consequently, the interpretation of results obtained from such studies must be approached with caution, as the genetic modifications can introduce confounding factors and influence neuronal mechanisms beyond the scope of AD-related research.

Indeed, the pathology of AD can be induced through various methods, as shown in Table 5. Some approaches include injecting $A\beta_{40}$ oligomers bilaterally into the hippocampus [65] or using $A\beta_{42}$ peptide [66]. In other studies, researchers induce the pathology using aluminum chloride [56] or a combination of aluminum chloride and D-galactose [57,58,60]. Another possibility involves the use of Streptozotocin, which induces autophagy [61,68–70]. Each of these methods offers valuable insights into different aspects of the disease's pathogenesis and helps researchers better understand its underlying mechanisms.

In all instances of inducing AD symptoms, the animals are categorized into groups to ensure a systematic evaluation. The first group serves as the control and receives no treatment. The second group is administered the inducing agent with varying amounts and for different durations (as indicated in Table 5). The third group is treated with both the inducing agent and the SeNPs under investigation. The data collected from these three groups are then subjected to statistical analysis using analysis of variance. This analytical approach allows researchers to assess the significance of differences between the groups and determine the effects of the inducing agent and SeNPs on the observed outcomes in a rigorous and quantitative manner.

4.1. Behavioral assays with mouse models of Alzheimer's disease

The hippocampus is a critical region for spatial memory, and early-stage AD can lead to damages in this area. When conducting studies with mice, it is essential to consider the differences between species. In humans, the hippocampus is associated with spatial and verbal memory, while in rodents, it is related to spatial navigation and olfactory behavior [105]. The Morris water maze test (MWM) is the most widely used method to evaluate how spatial cognitive behavior is affected by the disease and its treatment with SeNPs [57,58,60,64,65,75,76,83,85]. This test assesses learning and long-term spatial memory in mice. During the experiment, mice are trained for a variable duration, usually around five days, in a circular pool containing an escape platform positioned 1 cm below the water surface. During the initial training days, the mice are allowed a maximum time to locate the platform and can stay on it for a predetermined period. Following the training period, the platform is removed, and the mice are given the opportunity to swim freely. The number of times the mice cross the location where the platform used to be is recorded and subjected to statistical analysis. This analysis helps researchers to understand the impact of the disease and the potential therapeutic effects of SeNPs on spatial memory in the mice.

Regarding the treatment of transgenic mice with SeNPs, several strategies have been developed, as shown in Table 5. These strategies involve the use of chiral molecules, antioxidant polyphenolic compounds, peptides, or borneol to enhance passage through the BBB. For instance, transgenic mice were treated with capped to penicillamine chiral L-/D-Pen@SeNPs, resulting in a reduction in escape latency observed in all groups. However, animals treated with D-Pen@SeNPs exhibited a significant decrease in escape latency compared to those treated with L-Pen@SeNPs or the control group, highlighting the importance of the stereoselectivity of these NPs [76].

Similarly, the use of SeNPs modified with chlorogenic acid or with chlorogenic acid and TGN peptide [85] in APP/PS1 transgenic mice demonstrated significant cognitive improvement when treated with TGN-CGA@SeNCs. In contrast, no statistically significant improvements

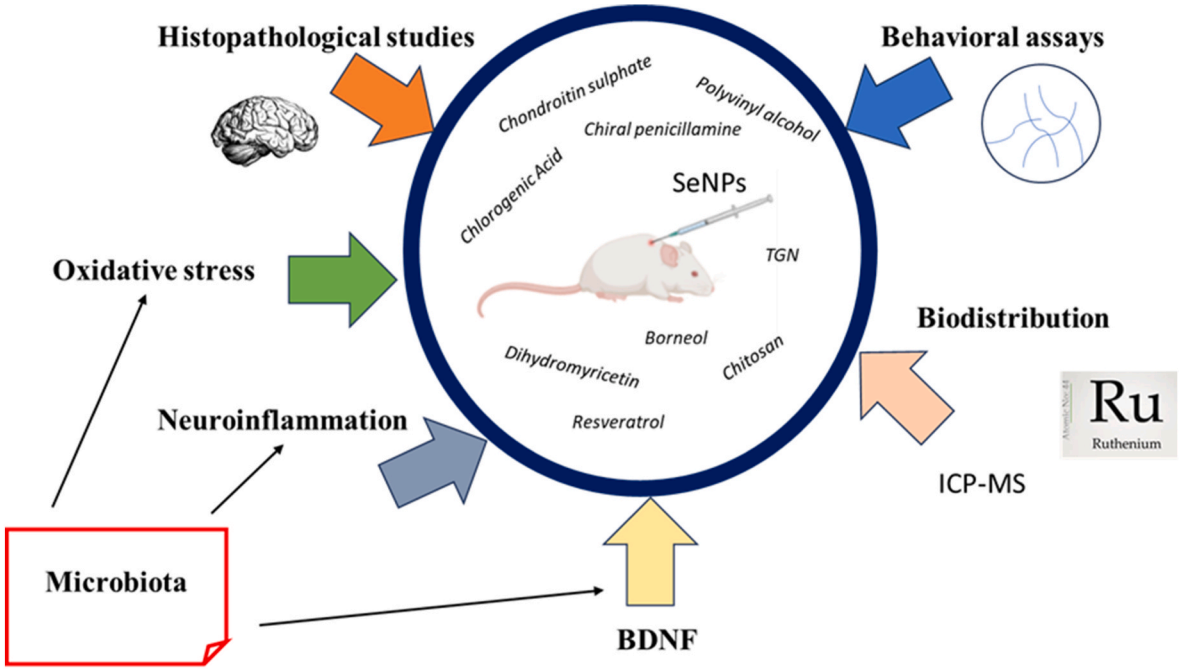

Fig. 6. Studies involving SeNPs for *in vivo* assays.

were observed when treated with CGA@SeNCs. Another attempt to improve the passage through the BBB involved modifying NPs with another polyphenol, dihydromyricetin, using the same peptide [75]. The study with CS/DMY@SeNPs and TGN-CS/DMY@SeNPs on the behavior of transgenic mice in the MWM trial showed that both NPs led to an improvement in cognitive ability.

Similar assays using resveratrol- and borneol-modified NPs have demonstrated improved memory impairment in APP/PS1 mice compared to untreated control mice [64]. Trials with transgenic mice have included the use of nanozyme with polydopamine modified with borneol [83]. The results from the MWM test revealed that mice treated with Se@PDA@Bor exhibited more frequent crossings over the location of the hidden platform and longer swim times, indicating an enhancement in cognitive ability and memory.

In addition to these studies, SeNPs modified with chondroitin sulphate CS@SeNPs [60], resveratrol-loaded selenium chitosan nano flowers Res@SeNPs@res–CS–NPs [58], and resveratrol-selenium-pep tide nanocomposites (TGN-Res@SeNPs) [57] have been employed in mice in which amyloid plaque formation was induced using D-galactose and aluminum chloride. In all these cases, improvements in spatial memory deficiency caused by D-galactose and AlCl3 were observed in mice after treatment with the different modified SeNPs. These findings indicate the potential therapeutic benefits of using SeNPs with various modifications for combating memory impairments associated with AD.

The novel object recognition (NOR) test has been employed in numerous studies involving both APP/PS1 transgenic mice [76,85] and mice in which AD symptoms were induced using a combination of D-galactose and aluminum chloride [60,61], $A\beta_{42}$ peptide [70], or streptozotocin [69].

In the NOR test [106], attention and visual recognition abilities are evaluated. The mice are introduced to a box without a lid and allowed to familiarize themselves with it for a predetermined time. Then, two identical objects are placed inside the box, and the curiosity displayed by the animals towards these objects is measured for a specific duration. On subsequent days, other objects of equivalent size but with different shapes are introduced, and the mice's behavior towards the new objects is again observed for a certain time. The results are expressed as a percentage of time spent exploring the new objects.

In the context of selenium nanoparticle treatments, certain observations have been made. Mice treated with L-Pen@SeNPs were unable to distinguish between new and familiar objects, whereas APP/PS1 mice treated with D-Pen@SeNPs demonstrated the ability to recognize the difference [76]. Similarly, in the case of treatment with CGA@SeNCs or TGN-CGA@SeNCs, only mice treated with TGN-CGA@SeNCs were able to distinguish new objects [85]. High doses of selenium nanoparticles modified with chondroitin sulphate CS@SeNPs showed improved results in the NOR test compared to the control group [60].

Combining SeNPs with stem cells (AMSCs) [61], SeNPs resulted in significant differences in the NOR test results compared to mice treated only with streptozotocin. Stem cell treatments combined with chitosan-coated nanoparticles (Ch-SeNPs) [70] also led to a decrease in cognitive impairment caused by streptozotocin, with greater enhancement observed when combined with Ch-SeNPs. Furthermore, cognitive abilities were increased in mice treated with selenium nanoparticles coated with polyvinyl alcohol (PVP-coated SeNPs) [69] after streptozotocin treatment.

Table 5 demonstrates that various tests can be utilized to evaluate different cognitive abilities in mice. These tests include the Open Field test [60,85], the Nesting test [83], the Y-maze spontaneous alternating test [66], and the Passive Avoidance Learning test [68]. Each of these tests offers distinct insights into various aspects of cognitive function and behavior in mice, providing valuable information for researchers studying AD and potential therapeutic interventions involving SeNPs.

4.2. Histopathological studies: effect of SeNPs in brain

After conducting behavioral studies, the animals are sacrificed, and their brains are examined to assess potential damage to the hippocampus and the presence of Aβ protein aggregates. These studies are conducted after fixing the brain tissues using various methods such as formaldehyde, glutaraldehyde, or paraffin embedding, among others [56,60,61,66,68–70,83]. The primary goal of histopathological studies is to determine the effects of SeNPs on symptoms such as edema, hypoplasia, neuronal degeneration, or the formation of amyloid plaques in the hippocampus.

To detect these modifications, various techniques may be employed, including microscope studies, photographic systems, or fluorescence measurements after appropriate treatment with a dye or fluorescent reagent. These methods enable the visualization and analysis of structural changes and molecular markers associated with AD, providing crucial insights into the potential therapeutic effects of SeNPs in mitigating pathological changes in the brain.

After hematoxylin-eosin staining, microscopic images of the CA1 zone of the hippocampus in mice treated with $AlCl_3$ display features indicative of edema, hypoplasia, neuronal degeneration, and amyloid plaques (at a x400 magnification). In contrast, mice administered RSV-SeNPs [56] exhibit higher neuronal density in the dentate gyrus and, overall, a healthier conformation of the CA1 region of the hippocampus.

In the study exploring the combined effect of stem cells with SeNPs or Ch-SeNPs [70], the cell tissue is stained with cresyl violet to assess cell density in the CA1 zone of the hippocampus. Congo red staining is employed to evaluate the presence of Aβ plaques. Light micrographs demonstrate that only the combination of AMSCs with Ch-SeNPs results in a significant decrease in Aβ plaque deposition.

In another study evaluating the effect of AMSCs conjugated with SeNPs, Congo red staining and analysis with ImageJ software revealed no significant differences in the number of plaques between mice treated and not treated with SeNPs. However, transplantation of AMSCs combined with SeNPs significantly reduced the number of plaques [61].

Optical microscopy, following Congo red staining, has also been employed to evaluate the effect of SeNPs on mice brains induced with AD using Streptozotocin. This approach demonstrated a reduction in the number of plaques in mice treated with SeNPs [68]. A similar methodology confirmed the beneficial effect of PVP-coated SeNPs on amyloid plaque degrowth [69].

TEM has been used to evaluate the formation of amyloid plaques in cell tissue [60]. This technique allows for the examination of hippocampal neuronal morphology, the number of synapses between neurons, and the morphology and structure of mitochondria in mice. Through TEM, it has been observed alterations in neurons of mice with AD, such as pyknosis, structural damage in synapses, reduction of postsynaptic density, or loss of activity. However, the brains of mice treated with nanoparticles modified with chondroitin sulphate (CS@SeNPs), particularly in medium and high doses, showed improvements in postsynaptic density, membrane disruption, and a reduction in mitochondrial swelling. Tissues were stained with lead citrate and uranyl acetate for this evaluation.

Additionally, the assessment of brain tissue with TUNEL immunofluorescence revealed a decrease in tau plaques in the brains of mice treated with SeCQDs [66]. This technique aids in evaluating the potential benefits of selenium quantum dots in reducing tau pathology, another characteristic feature of AD.

4.3. Biodistribution of selenium nanoparticles in mouse models

There are two main methods to evaluate the distribution of SeNPs: the first one is through ICP-MS analysis of the organs of the animals after they are sacrificed, and the second one involves chemically marking the NPs to track them in the body using imaging techniques.

ICP-MS analysis has been used to study the distribution of SeCQDs

[65] in different organs of mice treated with these NPs. SeCQDs were analyzed in the heart, liver, lungs, kidneys, spleen, and brain, and a high concentration of these NPs was observed in the brain, indicating their ability to cross the BBB. Similarly, the same technique was used with TGN-CS/DMY@SeNPs [75] to confirm their presence in mice brains and their ability to cross the BBB.

To assess the real-time mobility of NPs, researchers modified them with a fluorescent complex of Ru(II) and then injected the modified NPs into mice. NPs such as MSe-Ru2/Fc-β-CD/Bor [64] exhibited fluorescence in the brains of APP/PS1 mice within 15 min of injection. The maximum fluorescence intensity was reached 1 h after treatment, and fluorescent particles were primarily observed in the hippocampal dentate gyrus. Fluorescence was still present 12 h after treatment, indicating successful penetration through the BBB. This technique provides valuable insights into the ability of SeNPs to cross the BBB and their distribution within specific brain regions.

4.4. Bioanalytical assays: impact of selenium nanoparticles in mice

Several experimental studies involving SeNPs have a broader objective beyond assessing potential improvements in disease symptoms. They also strive to provide valuable information about the underlying molecular mechanisms associated with the dysfunctions observed in AD. Such research serves as a foundation for discovering innovative and effective therapeutic approaches against this debilitating condition.

4.4.1. Estimation of oxidative stress

The assessment of oxidative stress levels in the brain involves measuring malondialdehyde (MDA) levels and brain catalase activity (CAT). Mice treated with $AlCl_3$ exhibit severe tissue toxicity, leading to mitochondrial dysfunction and oxidative stress, resulting in reduced CAT activity and a significant increase in lipid oxidation (MDA). Conversely, mice treated with RSV-SeNPs [56] demonstrate reduced MDA levels and improved CAT activity compared to control mice that did not receive the NPs.

To further evaluate oxidative stress and antioxidant capacity, the total level of thiol groups (TTG) and total antioxidant capacity (TAC) in the hippocampal homogenate supernatant have been studied [68]. SeNPs enhance antioxidant capacity in the hippocampus by reducing MDA levels and increasing TTG levels relative to mice with AD symptoms [68]. Similarly, mice treated with PVP-coated SeNPs also show significant improvements in TAC and MDA levels [69]. These findings indicate that SeNPs have the potential to mitigate oxidative stress and enhance antioxidant defenses in the brain, providing valuable insights for potential therapeutic interventions against AD.

4.4.2. Estimation of anti-inflammatory effects

Neuroinflammation plays a critical role in the development of AD. Excessive production of Aβ and tau proteins triggers uncontrolled inflammation in brain tissues, leading to cell degeneration and death [104]. The presence of various cytokines, such as TNF-α, IL-1β, or IL-6, resulting from cellular inflation, can be evaluated through western blotting. Generally, AD mice exhibit high expression levels of TNF-α, IL-1β, and IL-6 proteins [60], which can be mitigated by CS@SeNPs treatments. Additionally, RSV-SeNPs reduce the expression of IL-1β protein and levels of the pSTAT3 gene, associated with inflammation, when compared to the control group [56].

By modifying NPs with the TGN peptide (TGN-Res@SeNPs), the production of TNF-α, IL-1β, and IL-6 can be reduced, while increasing the amount of IL-10, a protein that inhibits the overproduction of inflammatory cytokines by activating macrophages [57]. Treatment with TGN-CGA@SeNCs in transgenic mice also results in reduced overexpression of TNF-α, IL-1β, IL-18, and IL-6, with a simultaneous increase in IL-10 levels [85]. The presence of substances with antioxidant capacity in the NPs and the modification with the TGN peptide appear to enhance the anti-inflammatory effect of SeNPs.

These findings highlight the potential of SeNPs to modulate neuroinflammation in AD, offering a promising avenue for developing therapeutic interventions aimed at curbing inflammatory responses in the brain and potentially slowing the progression of the disease.

4.4.3. Estimation of brain-derived neurotrophic factor

Brain-derived neurotrophic factor (BDNF) is a crucial protein that promotes the generation of new brain cells and enhances the strength of existing ones. To assess BDNF levels, hippocampal tissue is homogenized with PBS and analyzed using an ELISA kit.

AMSCs SeNPs [61], AMSCs Ch-SeNPs [70], and PVP-coated SeNPs [69] induce an increase in the concentration of BDNF in the hippocampal region, resulting in an improved ability to repair damaged cells and even stimulate the generation of new cells. This enhancement in BDNF levels may play a vital role in potential therapeutic approaches for promoting neurodegeneration and neuroprotection in AD. By fostering the growth and maintenance of brain cells, SeNPs show promise in their potential to combat the neural degeneration associated with the disease and support the development of innovative treatment strategies.

4.4.4. Effects of selenium nanoparticles on microbiota

In recent years, research has begun to investigate the role of the microbiota in the development of AD. The human intestinal tract's microbiota comprises bacteria, viruses, fungi, and parasites [104]. Studies reveal a bidirectional relationship between the brain and gut microbiota through the nervous, endocrine, and immune systems. Changes in the composition of the microbiota, characterized by reduced diversity and stability, occur with age, as observed in feces and the microbiome of the small intestine [104]. Currently, the mechanisms linking AD and microbiota modification remain unknown, but microbiota dysbiosis appears to be associated with Aβ protein aggregation and neuroinflammation. Additionally, there seems to be a correlation between the BDNF factor, the N-methyl-D-aspartate receptor (NMDA), and a healthy microbiota.

Numerous studies have been conducted with SeNPs on microbial DNA from mouse feces using the Fast DNASpin kit. The V3–V4 region of the 16S rRNA gene is amplified with 338F and 806R primers via PCR analysis [57,75,85]. Evaluations of gut microbiota diversity and abundance, using the α-diversity index, indicate that mice treated with TGN-Res@SeNPs [57] demonstrate greater microbiota abundance and diversity. Mice with AD show an increased presence of pathogenic bacteria, such as *Alistipes* and *Rikenella*, while beneficial bacteria, like *Desulfovibrio*, are at lower levels. Treatment with TGN-Res@SeNPs results in an increase in beneficial bacteria and a reduction in pathogenic ones. A Spearman correlation study reveals a negative correlation between antioxidant capacity and some pathogenic bacteria, such as *Alistipes* and *Rikenella*, while a positive correlation is found between gut microbiota and inflammatory processes when the two aforementioned bacteria are combined. Treatment with TGN-Res@SeNPs leads to the restoration of the bacterium *Faecalibaculum* to normal levels and an increase in the amount of IL-10. Similarly, treatment with Rs@SeNPs@Res–CS–NPs [58] regulates the abundance of Firmicutes and Bacteroidetes, restoring the composition of the intestinal microbiota, and reducing inflammation, lipid deposition, and oxidative effects. Studies with CS/DMY@SeNPs [75] also show that improved microbiota regulation leads to the regulation of the NLRP3 inflammasome and an increase in the level of Bifidobacterium in mice.

These findings provide compelling evidence for the potential of SeNPs to influence gut microbiota and modulate inflammatory processes, contributing to a deeper understanding of the complex interactions between the microbiota and AD. Further research in this area holds promise for the development of targeted therapeutic interventions aimed at harnessing the gut-brain axis to combat neuroinflammation and enhance neuroprotection in AD.

5. Future trends in SeNPs for AD treatment: novel brain delivery strategies and expanding animal models

AD is a progressive neurodegenerative disorder that poses significant challenges in finding effective therapeutic interventions. In recent years, nanoparticle-based approaches, specifically SeNPs, have emerged as promising candidates for AD treatment. This section discusses future trends in SeNPs utilization for AD therapy, including innovations in brain delivery, alternative animal models for research, and unexplored areas for potential future trials.

The efficient delivery of therapeutic agents, including SeNPs, to the brain is hindered by the BBB. To overcome this challenge, efforts are well underway to develop novel brain delivery strategies that can traverse the BBB while minimizing toxicity. These advancements aim to enhance the accumulation of SeNPs within the brain parenchyma, where they can target AD pathology effectively. Promising approaches involve surface modifications with ligands that can interact with specific receptors expressed on BBB endothelial cells, enabling targeted transport of SeNPs into the brain. Additionally, the utilization of carrier systems, such as exosomes or liposomes, is being explored to enhance brain-specific delivery and reduce off-target effects.

While mouse models have been extensively employed in AD research, exploring alternative animal models can provide additional insights into disease mechanisms and therapeutic potential. *Caenorhabditis elegans* (*C. elegans*) and *Drosophila melanogaster* (fruit fly) are two species with fully sequenced genomes, therefore allowing to conduct detailed genetic and proteomic studies. Although these organisms differ significantly from humans, their genetic tractability and conserved signaling pathways related to AD may offer valuable information about the disease's underlying molecular processes and potential therapeutic targets. Integrating findings from these alternative models with data from mouse models could provide a more comprehensive understanding of AD pathogenesis and SeNPs efficacy.

Current AD research in mice often employs Al(III) to induce the disease, reflecting the aluminum hypothesis and its involvement in Aβ aggregation. However, the role of other metal ions, such as Fe(II), Cu(II) and Zn(II), in AD development remains an intriguing avenue for exploration. Considering the relevance of the "*metal ion hypothesis*", conducting *in vivo* studies to induce AD in animal models using iron, copper, and zinc could shed light on their potential contributions to AD pathology. Such investigations may reveal new avenues for SeNPs intervention based on their interaction with metal ions and amyloid aggregation processes.

Presently, the research on SeNPs frequently concentrates on a particular facet of AD pathology. However, AD is a multifaceted disorder with multiple underlying mechanisms. To maximize therapeutic efficacy, future studies could explore multi-targeted SeNPs formulations that simultaneously address key aspects of AD pathology, such as neuroinflammation, oxidative stress, and tau protein abnormalities. Such integrated approaches may yield synergistic effects and improve overall treatment outcomes. Further exploration of the interactions between SeNPs and gut microbiota is essential, as emerging evidence suggests a potential link between the microbiome and neuroprotection in AD treatment.

The future of SeNPs utilization for AD treatment holds immense promise. Innovations in brain delivery strategies, exploration of alternative animal models, investigations into metal-induced AD models, and multi-targeted formulations represent exciting areas for future research. Through the investigation and consideration of these aspects, noteworthy progress in comprehending the underlying causes of AD may be made. Moreover, this research can reveal the untapped possibilities of SeNPs as an innovative and promising therapeutic method for managing this severe neurodegenerative condition.

6. Conclusions

The present review explores the potential application of SeNPs in the treatment of AD while encompassing the diverse methods of SeNPs synthesis and the main bioanalytical techniques to assess the neuroprotective effect. AD, a progressive neurodegenerative disorder, is characterized by the accumulation of Aβ and tau proteins in the brain, leading to cognitive decline and neuronal damage.

The versatility of SeNPs in functionalization and their unique properties such as antioxidant capacity, anti-inflammatory effects, and BBB-penetrating ability, make them promising candidates for AD therapy. To fully harness their potential, different methods for SeNPs synthesis have been employed. SeNPs used in Alzheimer's disease studies are mainly produced by chemical approaches. However, green methods employing algae, yeast, plant extracts, fungi, and bacteria offer a promising, eco-friendly and biocompatible alternative for nanoparticle synthesis with potential therapeutic applications.

In vitro studies investigating the effects of SeNPs on AD have yielded encouraging results, demonstrating their ability to reduce amyloid aggregation, inhibit tau hyperphosphorylation, and mitigate oxidative stress-induced damage in neuronal cells. *In vivo* studies using transgenic mouse models and AD-induced symptoms have shown improvement in cognitive deficits and a reduction in amyloid plaque burden in the hippocampus upon SeNPs treatment.

However, challenges remain, particularly concerning the interpretation of data obtained from genetically modified mouse models due to potential confounding effects. To complement mouse studies, alternative animal models like *Caenorhabditis elegans* and *Drosophila melanogaster* are being explored, offering fully sequenced genomes and allowing for genetic and proteomic investigations related to AD.

Future trends in SeNPs utilization for AD treatment focus on innovative brain delivery strategies to overcome the BBB and enhance targeted delivery to the brain parenchyma. Surface modifications with ligands and carrier systems like exosomes and liposomes are being explored for this purpose. Moreover, multi-targeted SeNPs formulations addressing multiple aspects of AD pathology, including neuroinflammation, oxidative stress, and tau protein abnormalities, hold potential for synergistic therapeutic effects.

In conclusion, SeNPs represent a promising avenue for AD treatment due to their multifaceted properties and potential to address various aspects of AD pathogenesis. Diverse methods of SeNPs synthesis offer flexibility in tailoring nanoparticle characteristics. The combination of *in vitro* and *in vivo* studies with alternative animal models holds great promise for unravelling the complex mechanisms underlying AD and maximizing the therapeutic potential of SeNPs. As research in this area continues to advance, collaborative efforts across disciplines will pave the way for innovative therapeutic interventions that could revolutionize the management of Alzheimer's disease, alleviating the burden it poses on patients and caregivers worldwide.

CRediT authorship contribution statement

David Vicente-Zurdo: Conceptualization, Data curation, Investigation, Methodology, Writing – original draft, Writing – review & editing. **Noelia Rosales-Conrado:** Conceptualization, Methodology, Supervision, Writing – original draft, Writing – review & editing. **María Eugenia León-González:** Conceptualization, Methodology, Supervision, Writing – original draft, Writing – review & editing.

Declaration of competing interest

The authors declare that they have no known competing financial interests or personal relationships that could have appeared to influence the work reported in this paper.

Data availability

No data was used for the research described in the article.

Acknowledgments

The authors thank the Ministry of Science, Innovation and Universities (project PID 2020-114714RB-100) for the financial support.

Abbreviations

ACh	acetylcholine
AChE	acetylcholinesterase
AD	Alzheimer's disease
AMSCs	adipose mesenchymal stem cells
ANS	1-anilino-8-naphthalene sulphate
APP	amyloid precursor protein
Aβ	beta-amyloid
BBB	blood-brain barrier
BCh	butyrylcholine
BDNF	brain-derived neurotrophic factor
CAT	catalase
CGA	chlorogenic acid
CNS	central nervous system
DAPI	4′,6-diamidino-2-phenylindole
DCF	2′,7′-dichlorofluorescein
DCFH-DA	2′,7′-dichlorofluorescin diacetate
DLS	dynamic light scattering
DPPH	1,1-diphenyl-2-picrylhydrazyl
DSC	differential scanning calorimeter
ED	electron diffraction
EDX	energy-dispersive X-ray
EGCG	epigallocatechin-3-gallate
FTIR	Fourier transform infrared
GPx	glutathione peroxidases
HR-TEM	high-resolution transmission electron microscopy
ICP-MS	inductively coupled plasma mass spectrometry
LHD	lactate dehydrogenase
MDA	malondialdehyde
MMPs	matrix metalloproteases
MS	mass spectrometry
MSeNPs	mesoporous selenium nanoparticles
MTT	3-(4,5- dimethylthiazol-2-yl)-2,5-diphenyltetrazole bromide
MWM	Morris water maze test
Neuro-2a	mouse neuroblastoma cell line
NFTs	neurofibrillary tangles
NMDA	N-methyl-D-aspartate receptor
NOR	novel object recognition
NPs	nanoparticles
PC12	rat pheochromocytoma cell line
PI	propidium iodide
PLGA	poly-lactide-*co*-glycolide
p-tau	hyperphosphorylated tau protein
PVA	polyvinyl alcohol
QDs	quantum dots
Res	resveratrol
RLS	resonance light scattering
ROS	reactive oxygen species
SEM	scanning electron microscope
SeNCs	selenium nanocomposites
SeNPs	selenium nanoparticles
SH-SY5Y	human neuroblastoma cell line
TAC	total antioxidant capacity
TEM	transmission electron microscopy
ThT	Thioflavin T
TTG	total level of thiol groups
TUNEL	terminal deoxynucleotidyl transferase dUTP nick end labelling
XRD	X-ray diffraction

References

[1] J. Weller, A. Budson, Current understanding of Alzheimer's disease diagnosis and treatment, F1000Res 7 (2018) 1–9, https://doi.org/10.12688/f1000research.14506.1.
[2] V.L. Feigin, B. Norrving, G.A. Mensah, Global burden of stroke, Circ. Res. 120 (2017) 439–448, https://doi.org/10.1161/CIRCRESAHA.116.308413.
[3] M. Crous-Bou, C. Minguillón, N. Gramunt, J.L. Molinuevo, Alzheimer's disease prevention: from risk factors to early intervention, Alzheimer's Res. Ther. 9 (2017) 71, https://doi.org/10.1186/s13195-017-0297-z.
[4] C. Patterson, World Alzheimer Report 2018 - the State of the Art of Dementia Research: New Frontiers, Alzheimer Research International, 2018. https://www.alz.co.uk/research/world-report -2018. (Accessed 15 February 2022).
[5] Y. Hou, X. Dan, M. Babbar, Y. Wei, S.G. Hasselbalch, D.L. Croteau, V.A. Bohr, Ageing as a risk factor for neurodegenerative disease, Nat. Rev. Neurol. 15 (2019) 565–581, https://doi.org/10.1038/s41582-019-0244-7.
[6] Alzheimer's Disease International, World Alzheimer Report 2021, 2021. https://www.alzint.org/resource/world-alzheimer-report-2021/. (Accessed 20 February 2022).
[7] E. Ray Dorsey, A. Elbaz, E. Nichols, F. Abd-Allah, A. Abdelalim, J.C. Adsuar, M. G. Ansha, C. Brayne, J.Y.J. Choi, D. Collado-Mateo, N. Dahodwala, H.P. Do, D. Edessa, M. Endres, S.M. Fereshtehnejad, K.J. Foreman, F.G. Gankpe, R. Gupta, G.J. Hankey, S.I. Hay, M.I. Hegazy, D.T. Hibstu, A. Kasaeian, Y. Khader, I. Khalil, Y.H. Khang, Y.J. Kim, Y. Kokubo, G. Logroscino, J. Massano, N.M. Ibrahim, M. A. Mohammed, A. Mohammadi, M. Moradi-Lakeh, M. Naghavi, B.T. Nguyen, Y. L. Nirayo, F.A. Ogbo, M.O. Owolabi, D.M. Pereira, M.J. Postma, M. Qorbani, M. A. Rahman, K.T. Roba, H. Safari, S. Safiri, M. Satpathy, M. Sawhney, A. Shafieesabet, M.S. Shiferaw, M. Smith, C.E.I. Szoeke, R. Tabarés-Seisdedos, N. T. Truong, K.N. Ukwaja, N. Venketasubramanian, S. Villafaina, K. G. Weldegwergs, R. Westerman, T. Wijeratne, A.S. Winkler, B.T. Xuan, N. Yonemoto, V.L. Feigin, T. Vos, C.J.L. Murray, Global, regional, and national burden of Parkinson's disease, 1990–2016: a systematic analysis for the Global Burden of Disease Study 2016, Lancet Neurol. 17 (2018) 939–953, https://doi.org/10.1016/S1474-4422(18)30295-3.
[8] J.P. Taylor, R.H. Brown, D.W. Cleveland, Decoding ALS: from genes to mechanism, Nature 539 (2016) 197–206, https://doi.org/10.1038/nature20413.
[9] P. McColgan, S.J. Tabrizi, Huntington's disease: a clinical review, Eur. J. Neurol. 25 (2018) 24–34, https://doi.org/10.1111/ene.13413.
[10] H. Keren-Shaul, A. Spinrad, A. Weiner, O. Matcovitch-Natan, R. Dvir-Szternfeld, T.K. Ulland, E. David, K. Baruch, D. Lara-Astaiso, B. Toth, S. Itzkovitz, M. Colonna, M. Schwartz, I. Amit, A unique microglia type associated with restricting development of alzheimer's disease, Cell 169 (2017) 1276–1290, https://doi.org/10.1016/j.cell.2017.05.018.
[11] I. Agrawal, S. Jha, Mitochondrial dysfunction and alzheimer's disease: role of microglia, Front. Aging Neurosci. 12 (2020) 1–8, https://doi.org/10.3389/fnagi.2020.00252.
[12] Alzheimer's Association, 2020 Alzheimer's disease facts and figures, Alzheimer's Dementia 16 (2020) 391–460, https://doi.org/10.1002/alz.12068.
[13] H.R. Brunnström, E.M. Englund, Cause of death in patients with dementia disorders, Eur. J. Neurol. 16 (2009) 488–492, https://doi.org/10.1111/j.1468-1331.2008.02503.x.
[14] P. Davies, A.J. Maloney, Selective loss of central cholinergic neurons in Alzheimer's disease, Lancet 2 (1976) 1403, https://doi.org/10.1016/s0140-6736(76)91936-x.
[15] A. Sanabria-Castro, I. Alvarado-Echeverría, C. Monge-Bonilla, Molecular pathogenesis of alzheimer's disease: an update, Ann. Neurosci. 24 (2017) 46–54, https://doi.org/10.1159/000464422.
[16] M. Tang, C. Taghibiglou, J. Liu, The mechanisms of action of curcumin in alzheimer's disease, J. Alzheim. Dis. 58 (2017) 1003–1016, https://doi.org/10.3233/JAD-170188.
[17] T.H. Ferreira-Vieira, I.M. Guimaraes, F.R. Silva, F.M. Ribeiro, Alzheimer's disease: targeting the cholinergic system, Curr. Neuropharmacol. 14 (2016) 101–115, https://doi.org/10.2174/1570159x13666150716165726.
[18] W.J. Deardorff, E. Feen, G.T. Grossberg, The use of cholinesterase inhibitors across all stages of alzheimer's disease, Drugs Aging 32 (2015) 537–547, https://doi.org/10.1007/s40266-015-0273-x.
[19] J. Hardy, D. Allsop, Amyloid deposition as the central event in the aetiology of Alzheimer's disease, Trends Pharmacol. Sci. 12 (1991) 383–388, https://doi.org/10.1016/0165-6147(91)90609-V.
[20] P.P. Liu, Y. Xie, X.Y. Meng, J.S. Kang, History and progress of hypotheses and clinical trials for Alzheimer's disease, Signal Transduct. Targeted Ther. 4 (2019) 29, https://doi.org/10.1038/s41392-019-0063-8.
[21] E. Karran, B. De Strooper, The amyloid cascade hypothesis: are we poised for success or failure? J. Neurochem. 139 (2016) 237–252, https://doi.org/10.1111/jnc.13632.
[22] P.R. Angelova, A.Y. Abramov, Role of mitochondrial ROS in the brain: from physiology to neurodegeneration, FEBS Lett. 592 (2018) 692–702, https://doi.org/10.1002/1873-3468.12964.
[23] C. Bacchella, S. Gentili, D. Bellotti, E. Quartieri, S. Draghi, M.C. Baratto, M. Remelli, D. Valensin, E. Monzani, S. Nicolis, L. Casella, M. Tegoni,

S. Dell'Acqua, Binding and reactivity of copper to R1 and R3 fragments of tau protein, Inorg. Chem. 59 (2020) 274–286, https://doi.org/10.1021/acs.inorgchem.9b02266.
[24] E.E. Congdon, E.M. Sigurdsson, Tau-targeting therapies for Alzheimer disease, Nat. Rev. Neurol. 14 (2018) 399–415, https://doi.org/10.1038/s41582-018-0013-z.
[25] A. Lučiūnaitė, R.M. McManus, M. Jankunec, I. Rácz, C. Dansokho, I. Dalgėdienė, S. Schwartz, F. Brosseron, M.T. Heneka, Soluble Aβ oligomers and protofibrils induce NLRP3 inflammasome activation in microglia, J. Neurochem. 155 (2020) 650–661, https://doi.org/10.1111/jnc.14945.
[26] S.E. Nasrabady, B. Rizvi, J.E. Goldman, A.M. Brickman, White matter changes in Alzheimer's disease: a focus on myelin and oligodendrocytes, Acta Neuropathol Commun 6 (2018) 22, https://doi.org/10.1186/s40478-018-0515-3.
[27] Alzheimer's Association, 2018 Alzheimer's disease facts and figures, Alzheimer's Dementia 14 (2018) 367–429, https://doi.org/10.1016/j.jalz.2018.02.001.
[28] C.A. Lane, J. Hardy, J.M. Schott, Alzheimer's disease, Eur. J. Neurol. 25 (2018) 59–70, https://doi.org/10.1111/ene.13439.
[29] T.J. Huat, J. Camats-Perna, E.A. Newcombe, N. Valmas, M. Kitazawa, R. Medeiros, Metal toxicity links to alzheimer's disease and neuroinflammation, J. Mol. Biol. 431 (2019) 1843–1868, https://doi.org/10.1016/j.jmb.2019.01.018.
[30] L.L. Chen, Y.G. Fan, L.X. Zhao, Q. Zhang, Z.Y. Wang, The metal ion hypothesis of Alzheimer's disease and the anti-neuroinflammatory effect of metal chelators, Bioorg. Chem. 131 (2023), 106301, https://doi.org/10.1016/j.bioorg.2022.106301.
[31] E.L. Que, D.W. Domaille, C.J. Chang, Metals in neurobiology: probing their chemistry and biology with molecular imaging, Chem. Rev. 108 (2008) 1517–1549, https://doi.org/10.1021/cr800447y.
[32] Y. Liu, M. Nguyen, A. Robert, B. Meunier, Metal ions in alzheimer's disease: a key role or not? Acc. Chem. Res. 52 (2019) 2026–2035, https://doi.org/10.1021/acs.accounts.9b00248.
[33] F. Davarani Asl, M. Mousazadeh, M. Azimzadeh, M.R. Ghaani, Mesoporous selenium nanoparticles for therapeutic goals: a review, J. Nanoparticle Res. 24 (2022), https://doi.org/10.1007/s11051-022-05572-7.
[34] F. Gao, J. Zhao, P. Liu, D. Ji, L. Zhang, M. Zhang, Y. Li, Y. Xiao, Preparation and in vitro evaluation of multi-target-directed selenium-chondroitin sulfate nanoparticles in protecting against the Alzheimer's disease, Int. J. Biol. Macromol. 142 (2020) 265–276, https://doi.org/10.1016/j.ijbiomac.2019.09.098.
[35] S. Menon, V.K. Shanmugam, Chemopreventive mechanism of action by oxidative stress and toxicity induced surface decorated selenium nanoparticles, J. Trace Elem. Med. Biol. 62 (2020), 126549, https://doi.org/10.1016/j.jtemb.2020.126549.
[36] Z.H. Zhang, L. Wen, Q.Y. Wu, C. Chen, R. Zheng, Q. Liu, J.Z. Ni, G.L. Song, Long-term dietary supplementation with selenium-enriched yeast improves cognitive impairment, reverses synaptic deficits, and mitigates tau pathology in a triple transgenic mouse model of alzheimer's disease, J. Agric. Food Chem. 65 (2017) 4970–4979, https://doi.org/10.1021/acs.jafc.7b01465.
[37] M. Soriano-Garcia, Organoselenium compounds as potential therapeutic and chemopreventive agents: a review, Curr. Med. Chem. 11 (2012) 1657–1669, https://doi.org/10.2174/0929867043365053.
[38] T.G. Sors, C.P. Martin, D.E. Salt, Characterization of selenocysteine methyltransferases from Astragalus species with contrasting selenium accumulation capacity, Plant J. 59 (2009) 110–122, https://doi.org/10.1111/j.1365-313X.2009.03855.x.
[39] A.S. Rahmanto, M.J. Davies, Selenium-containing amino acids as direct and indirect antioxidants, IUBMB Life 64 (2012) 863–871, https://doi.org/10.1002/iub.1084.
[40] M.A. Ismael, A.M. Elyamine, M.G. Moussa, M. Cai, X. Zhao, C. Hu, Cadmium in plants: uptake, toxicity, and its interactions with selenium fertilizers, Metallomics 11 (2019) 255–277, https://doi.org/10.1039/c8mt00247a.
[41] M.M. Rahman, K.F.B. Hossain, S. Banik, M.T. Sikder, M. Akter, S.E.C. Bondad, M. S. Rahaman, T. Hosokawa, T. Saito, M. Kurasaki, Selenium and zinc protections against metal-(loids)-induced toxicity and disease manifestations: a review, Ecotoxicol. Environ. Saf. 168 (2019) 146–163, https://doi.org/10.1016/j.ecoenv.2018.10.054.
[42] I. Zwolak, The role of selenium in arsenic and cadmium toxicity: an updated review of scientific literature, Biol. Trace Elem. Res. 193 (2020) 44–63, https://doi.org/10.1007/s12011-019-01691.
[43] J. Feldmann, A. Elgazali, M.F. Ezzeldin, Z. Gajdosechova, E. Krupp, F. Aborode, M.M. Lawan, A. Raab, A.H. Petursdottir, K. Amayo, Microwave-assisted sample preparation for element speciation, in: Microwave-Assisted Sample Preparation for Trace Element Determination, Elsevier, 2014, pp. 281–312, https://doi.org/10.1016/B978-0-444-59420-4.00010-6.
[44] H.W. Tan, H.Y. Mo, A.T.Y. Lau, Y.M. Xu, Selenium species: current status and potentials in cancer prevention and therapy, Int. J. Mol. Sci. 20 (2019) 1–26, https://doi.org/10.3390/ijms20010075.
[45] S.A. Wadhwani, U.U. Shedbalkar, R. Singh, B.A. Chopade, Biogenic selenium nanoparticles: current status and future prospects, Appl. Microbiol. Biotechnol. 100 (2016) 2555–2566, https://doi.org/10.1007/s00253-016-7300-7.
[46] J. Gupta, M.T. Fatima, Z. Islam, R.H. Khan, V.N. Uversky, P. Salahuddin, Nanoparticle formulations in the diagnosis and therapy of Alzheimer's disease, Int. J. Biol. Macromol. 130 (2019) 515–526, https://doi.org/10.1016/j.ijbiomac.2019.02.156.
[47] A. Khurana, S. Tekula, M.A. Saifi, P. Venkatesh, C. Godugu, Therapeutic applications of selenium nanoparticles, Biomed. Pharmacother. 111 (2019) 802–812, https://doi.org/10.1016/j.biopha.2018.12.146.
[48] C.M. Sims, S.K. Hanna, D.A. Heller, C.P. Horoszko, M.E. Johnson, A.R. Montoro Bustos, V. Reipa, K.R. Riley, B.C. Nelson, Redox-active nanomaterials for nanomedicine applications, Nanoscale 9 (2017) 15226–15251, https://doi.org/10.1039/c7nr05429g.
[49] L. Yang, J. Sun, W. Xie, Y. Liu, J. Liu, Dual-functional selenium nanoparticles bind to and inhibit amyloid β fiber formation in Alzheimer's disease, J. Mater. Chem. B 5 (2017) 5954–5967, https://doi.org/10.1039/c6tb02952c.
[50] C. Ferro, H.F. Florindo, H.A. Santos, Selenium nanoparticles for biomedical applications: from development and characterization to therapeutics, Adv. Healthcare Mater. 10 (2021), https://doi.org/10.1002/adhm.202100598.
[51] N. Bisht, P. Phalswal, P.K. Khanna, Selenium nanoparticles: a review on synthesis and biomedical applications, Mater Adv 3 (2022) 1415–1431, https://doi.org/10.1039/d1ma00639h.
[52] T.M. Sakr, M. Korany, K.V. Katti, Selenium nanomaterials in biomedicine—an overview of new opportunities in nanomedicine of selenium, J. Drug Deliv. Sci. Technol. 46 (2018) 223–233, https://doi.org/10.1016/j.jddst.2018.05.023.
[53] H. Ashraf, D. Cossu, S. Ruberto, M. Noli, S. Jasemi, E.R. Simula, L.A. Sechi, Latent potential of multifunctional selenium nanoparticles in neurological diseases and altered gut microbiota, Materials 16 (2023), https://doi.org/10.3390/ma16020699.
[54] L. Qiao, Y. Chen, X. Song, X. Dou, C. Xu, Selenium nanoparticles-enriched Lactobacillus casei ATCC 393 prevents cognitive dysfunction in mice through modulating microbiota-gut-brain Axis, Int. J. Nanomed. 17 (2022) 4807–4827, https://doi.org/10.2147/IJN.S374024.
[55] L. Yang, W. Wang, J. Chen, N. Wang, G. Zheng, A comparative study of resveratrol and resveratrol-functional selenium nanoparticles: inhibiting amyloid β aggregation and reactive oxygen species formation properties, J. Biomed. Mater. Res. 106 (2018) 3034–3041, https://doi.org/10.1002/jbm.a.36493.
[56] O.A.R. Abozaid, M.W. Sallam, S. El-Sonbaty, S. Aziza, B. Emad, E.S.A. Ahmed, Resveratrol-selenium nanoparticles alleviate neuroinflammation and neurotoxicity in a rat model of alzheimer's disease by regulating sirt1/miRNA-134/gsk3β expression, Biol. Trace Elem. Res. 200 (2022) 5104–5114, https://doi.org/10.1007/s12011-021-03073-7.
[57] C. Li, N. Wang, G. Zheng, L. Yang, Oral administration of resveratrol-selenium-peptide nanocomposites alleviates alzheimer's disease-like pathogenesis by inhibiting Aβ aggregation and regulating gut microbiota, ACS Appl. Mater. Interfaces 13 (2021) 46406–46420, https://doi.org/10.1021/acsami.1c14818.
[58] L. Yang, Y. Wang, G. Zheng, Z. Li, J. Mei, Resveratrol-loaded selenium/chitosan nano-flowers alleviate glucolipid metabolism disorder-associated cognitive impairment in Alzheimer's disease, Int. J. Biol. Macromol. 239 (2023), https://doi.org/10.1016/j.ijbiomac.2023.124316.
[59] T. Yin, L. Yang, Y. Liu, X. Zhou, J. Sun, J. Liu, Sialic acid (SA)-modified selenium nanoparticles coated with a high blood-brain barrier permeability peptide-B6 peptide for potential use in Alzheimer's disease, Acta Biomater. 25 (2015) 172–183, https://doi.org/10.1016/j.actbio.2015.06.035.
[60] D. Ji, X. Wu, D. Li, P. Liu, S. Zhang, D. Gao, F. Gao, M. Zhang, Y. Xiao, Protective effects of chondroitin sulphate nano-selenium on a mouse model of Alzheimer's disease, Int. J. Biol. Macromol. 154 (2020) 233–245, https://doi.org/10.1016/j.ijbiomac.2020.03.079.
[61] B. Gholamigeravand, S. Shahidi, S. Afshar, P. Gholipour, A. Samzadeh-kermani, K. Amiri, M. Majidi, R. Abbasalipourkabir, M.R. Arabestani, S. Soleimani Asl, Synergistic effects of adipose-derived mesenchymal stem cells and selenium nanoparticles on streptozotocin-induced memory impairment in the rat, Life Sci. 272 (2021), https://doi.org/10.1016/j.lfs.2021.119246.
[62] L. Yang, N. Wang, G. Zheng, Enhanced effect of combining chlorogenic acid on selenium nanoparticles in inhibiting amyloid β aggregation and reactive oxygen species formation in vitro, Nanoscale Res. Lett. 13 (2018), https://doi.org/10.1186/s11671-018-2720-1.
[63] V. Saini, A. Singh, R. Shukla, K. Jain, A.K. Yadav, Silymarin-Encapsulated xanthan gum–stabilized selenium nanocarriers for enhanced activity against amyloid fibril cytotoxicity, AAPS PharmSciTech 23 (2022), https://doi.org/10.1208/s12249-022-02274-0.
[64] J. Sun, C. Wei, Y. Liu, W. Xie, M. Xu, H. Zhou, J. Liu, Progressive release of mesoporous nano-selenium delivery system for the multi-channel synergistic treatment of Alzheimer's disease, Biomaterials 197 (2019) 417–431, https://doi.org/10.1016/j.biomaterials.2018.12.027.
[65] X. Zhou, S. Hu, S. Wang, Y. Pang, Y. Lin, M. Li, Large amino acid mimicking selenium-doped carbon quantum dots for multi-target therapy of alzheimer's disease, Front. Pharmacol. 12 (2021), https://doi.org/10.3389/fphar.2021.778613.
[66] X. Guo, Q. Lie, Y. Liu, Z. Jia, Y. Gong, X. Yuan, J. Liu, Multifunctional selenium quantum dots for the treatment of alzheimer's disease by reducing aβ-neurotoxicity and oxidative stress and alleviate neuroinflammation, ACS Appl. Mater. Interfaces 13 (2021) 30261–30273, https://doi.org/10.1021/acsami.1c00690.
[67] M.C. Zambonino, E.M. Quizhpe, L. Mouheb, A. Rahman, S.N. Agathos, S. A. Dahoumane, Biogenic selenium nanoparticles in biomedical sciences: properties, current trends, novel opportunities and emerging challenges in theranostic nanomedicine, Nanomaterials 13 (2023), https://doi.org/10.3390/nano13030424.
[68] B. Gholamigeravand, S. Shahidi, I. Amiri, A. Samzadeh-kermani, R. Abbasalipourkabir, S. Soleimani Asl, Administration of selenium nanoparticles

reverses streptozotocin-induced neurotoxicity in the male rats, Metab. Brain Dis. 36 (2021) 1259–1266, https://doi.org/10.1007/s11011-021-00713-8.
[69] N. Hashemi-Firouzi, S. Afshar, S.S. Asl, A. Samzadeh-Kermani, B. Gholamigeravand, K. Amiri, M. Majidi, S. Shahidi, The effects of polyvinyl alcohol-coated selenium nanoparticles on memory impairment in rats, Metab. Brain Dis. 37 (2022) 3011–3021, https://doi.org/10.1007/s11011-022-01084-4.
[70] S. Soleimani Asl, I. Amiri, A. Samzadeh- kermani, R. Abbasalipourkabir, B. Gholamigeravand, S. Shahidi, Chitosan-coated Selenium nanoparticles enhance the efficiency of stem cells in the neuroprotection of streptozotocin-induced neurotoxicity in male rats, Int. J. Biochem. Cell Biol. 141 (2021), https://doi.org/10.1016/j.biocel.2021.106089.
[71] D. Vicente-Zurdo, I. Romero-Sánchez, N. Rosales-Conrado, M.E. León-González, Y. Madrid, Ability of selenium species to inhibit metal-induced Aβ aggregation involved in the development of Alzheimer's disease, Anal. Bioanal. Chem. 412 (2020) 6485–6497, https://doi.org/10.1007/s00216-020-02644-2.
[72] D. Vicente-Zurdo, S. Rodríguez-Blázquez, E. Gómez-Mejía, N. Rosales-Conrado, M.E. León-González, Y. Madrid, Neuroprotective activity of selenium nanoparticles against the effect of amino acid enantiomers in Alzheimer's disease, Anal. Bioanal. Chem. 414 (2022) 7573–7584, https://doi.org/10.1007/s00216-022-04285-z.
[73] D. Vicente-Zurdo, B. Gómez-Gómez, I. Romero-Sánchez, N. Rosales-Conrado, M. E. León-González, Y. Madrid, Cytotoxicity, uptake and accumulation of selenium nanoparticles and other selenium species in neuroblastoma cell lines related to Alzheimer's disease by using cytotoxicity assays, TEM and single cell-ICP-MS, Anal. Chim. Acta 1249 (2023), https://doi.org/10.1016/j.aca.2023.340949.
[74] J. Zhang, X. Zhou, Q. Yu, L. Yang, D. Sun, Y. Zhou, J. Liu, Epigallocatechin-3-gallate (EGCG)-stabilized selenium nanoparticles coated with Tet-1 peptide to reduce amyloid-β aggregation and cytotoxicity, ACS Appl. Mater. Interfaces 6 (2014) 8475–8487, https://doi.org/10.1021/am501341u.
[75] L. Yang, Y. Cui, H. Liang, Z. Li, N. Wang, Y. Wang, G. Zheng, Multifunctional selenium nanoparticles with different surface modifications ameliorate neuroinflammation through the gut microbiota-NLRP3 inflammasome-brain Axis in APP/PS1 mice, ACS Appl. Mater. Interfaces 14 (2022) 30557–30570, https://doi.org/10.1021/acsami.2c06283.
[76] D. Sun, W. Zhang, Q. Yu, X. Chen, M. Xu, Y. Zhou, J. Liu, Chiral penicillamine-modified selenium nanoparticles enantioselectively inhibit metal-induced amyloid β aggregation for treating Alzheimer's disease, J. Colloid Interface Sci. 505 (2017) 1001–1010, https://doi.org/10.1016/j.jcis.2017.06.083.
[77] S.Y. Al-Qaraleh, W.A. Al-Zereini, S.A. Oran, Phyto-decoration of selenium nanoparticles using Moringa peregrina (forssk.) fiori aqueous extract: chemical characterization and bioactivity evaluation, Biointerface Res Appl Chem 13 (2023), https://doi.org/10.33263/BRIAC132.112.
[78] M. Borowska, J. Jiménez-Lamana, K. Bierla, K. Jankowski, J. Szpunar, A green and fast microwave-assisted synthesis of selenium nanoparticles and their characterization under gastrointestinal conditions using mass spectrometry, Food Chem. 417 (2023), https://doi.org/10.1016/j.foodchem.2023.135864.
[79] L. González-Salitre, A. Castañeda-Ovando, U.A. Basilio-Cortés, A. del Carmen García-Contreras, G.M. Rodríguez Serrano, A. Cardelle-Cobas, A.D. Román-Gutiérrez, L.G. González-Olivares, Biogenic production of seleno-amino acids and seleno-nanoparticles by Saccharomyces boulardii, Food Biosci. 53 (2023), 102552, https://doi.org/10.1016/j.fbio.2023.102552.
[80] L. Qiao, Y. Chen, X. Dou, X. Song, C. Xu, Biogenic selenium nanoparticles attenuate aβ25–35-induced toxicity in PC12 cells via Akt/CREB/BDNF signaling pathway, Neurotox. Res. 40 (2022) 1869–1881, https://doi.org/10.1007/s12640-022-00590-8.
[81] N. Satarzadeh, A. Sadeghi Dousari, B. Amirheidari, M. Shakibaie, A. Ramezani Sarbandi, H. Forootanfar, An insight into biofabrication of selenium nanostructures and their biomedical application, 3 Biotech 13 (2023), https://doi.org/10.1007/s13205-023-03476-4.
[82] X. Huo, Y. Zhang, X. Jin, Y. Li, L. Zhang, A novel synthesis of selenium nanoparticles encapsulated PLGA nanospheres with curcumin molecules for the inhibition of amyloid β aggregation in Alzheimer's disease, J. Photochem. Photobiol., B 190 (2019) 98–102, https://doi.org/10.1016/j.jphotobiol.2018.11.008.
[83] Y. Gong, A. Huang, X. Guo, Z. Jia, X. Chen, X. Zhu, Y. Xia, J. Liu, Y. Xu, X. Qin, Selenium-core nanozymes dynamically regulates Aβ & neuroinflammation circulation: augmenting repair of nervous damage, Chem. Eng. J. 418 (2021), https://doi.org/10.1016/j.cej.2021.129345.
[84] Y. Qi, P. Yi, T. He, X. Song, Y. Liu, Q. Li, J. Zheng, R. Song, C. Liu, Z. Zhang, W. Peng, Y. Zhang, Quercetin-loaded selenium nanoparticles inhibit amyloid-β aggregation and exhibit antioxidant activity, Colloids Surf. A Physicochem. Eng. Asp. 602 (2020) 125058–125067, https://doi.org/10.1016/j.colsurfa.2020.125058.
[85] Z. Li, G. Zheng, N. Wang, H. Liang, C. Li, Y. Wang, Y. Cui, L. Yang, A flower-like brain targeted selenium nanocluster lowers the chlorogenic acid dose for ameliorating cognitive impairment in APP/PS1 mice, J. Agric. Food Chem. 71 (2023) 2883–2897, https://doi.org/10.1021/acs.jafc.2c06809.
[86] R.S. Oremland, M.J. Herbel, J.S. Blum, S. Langley, T.J. Beveridge, P.M. Ajayan, T. Sutto, A.V. Ellis, S. Curran, Structural and spectral features of selenium nanospheres produced by Se-respiring bacteria, Appl. Environ. Microbiol. 70 (2004) 52–60, https://doi.org/10.1128/AEM.70.1.52-60.2004.
[87] J. Dobias, E.I. Suvorova, R. Bernier-Latmani, Role of proteins in controlling selenium nanoparticle size, Nanotechnology 22 (2011), 195605, https://doi.org/10.1088/0957-4484/22/19/195605.
[88] P.J. Fesharaki, P. Nazari, M. Shakibaie, S. Rezaie, M. Banoee, M. Abdollahi, A. R. Shahverdi, Biosynthesis of selenium nanoparticles using Klebsiella pneumoniae and their recovery by a simple sterilization process, Braz. J. Microbiol. 41 (2010) 461–466, https://doi.org/10.1590/S1517-83822010000200028.
[89] S. Sasidharan, R. Balakrishnaraja, Comparison studies on the synthesis of selenium nanoparticles by various micro-organisms, Int. J. Pure App. Biosci. 2 (2014) 112–117. http://www.ijpab.com/form/2014 Volume 2, issue 1/IJPAB-2014-2-1-112-117.pdf.
[90] G. Sharma, A.R. Sharma, R. Bhavesh, J. Park, B. Ganbold, J.S. Nam, S.S. Lee, Biomolecule-mediated synthesis of selenium nanoparticles using dried vitis vinifera (raisin) extract, Molecules 19 (2014) 2761–2770, https://doi.org/10.3390/molecules19032761.
[91] C.H. Ramamurthy, K.S. Sampath, P. Arunkumar, M.S. Kumar, V. Sujatha, K. Premkumar, C. Thirunavukkarasu, Green synthesis and characterization of selenium nanoparticles and its augmented cytotoxicity with doxorubicin on cancer cells, Bioproc. Biosyst. Eng. 36 (2013) 1131–1139, https://doi.org/10.1007/s00449-012-0867-1.
[92] K.S. Prasad, K. Selvaraj, Biogenic synthesis of selenium nanoparticles and their effect on as(III)-induced toxicity on human lymphocytes, Biol. Trace Elem. Res. 157 (2014) 275–283, https://doi.org/10.1007/s12011-014-9891-0.
[93] A. Kumar, K.S. Prasad, Role of nano-selenium in health and environment, J. Biotechnol. 325 (2021) 152–163, https://doi.org/10.1016/j.jbiotec.2020.11.004.
[94] M. Abbas, Potential role of nanoparticles in treating the accumulation of amyloid-beta peptide in alzheimer's patients, Polymers 13 (2021) 1051–1085, https://doi.org/10.3390/polym13071051.
[95] M. Yu, X. Chen, J. Liu, Q. Ma, Z. Zhuo, H. Chen, L. Zhou, S. Yang, L. Zheng, C. Ning, J. Xu, T. Gao, S.T. Hou, Gallic acid disruption of Aβ1–42 aggregation rescues cognitive decline of APP/PS1 double transgenic mouse, Neurobiol. Dis. 124 (2019) 67–80, https://doi.org/10.1016/j.nbd.2018.11.009.
[96] M.R. Nilsson, Techniques to study amyloid fibril formation in vitro, Methods 34 (2004) 151–160, https://doi.org/10.1016/j.ymeth.2004.03.012.
[97] N. Moreno, Image processing with ImageJ, Biophot. Int. 11 (2007) 249–258, https://doi.org/10.1201/9781420005615.ax4.
[98] Z. Bian, C. Cao, J. Ding, L. Ding, S. Yu, C. Zhang, Q. Liu, L. Zhu, J. Li, Y. Zhang, Y. Liu, Neuroprotective effects of PRG on Aβ25-35-induced cytotoxicity through activation of the ERK1/2 signaling pathway, J. Ethnopharmacol. 313 (2023), 116550, https://doi.org/10.1016/j.jep.2023.116550.
[99] S. Soleimani Asl, A. Gharebaghi, S. Shahidi, S. Afshar, F. Kalhori, K. Amiri, F. Mirzaei, Deferoxamine preconditioning enhances the protective effects of stem cells in streptozotocin-induced Alzheimer's disease, Life Sci. 287 (2021), 120093, https://doi.org/10.1016/j.lfs.2021.120093.
[100] D. Vicente-Zurdo, N. Rosales-Conrado, M.E. León-González, L. Brunetti, L. Piemontese, A. Raquel Pereira-Santos, S.M. Cardoso, Y. Madrid, S. Chaves, M. A. Santos, Novel rivastigmine derivatives as promising multi-target compounds for potential treatment of alzheimer's disease, Biomedicines 10 (2022) 1510, https://doi.org/10.3390/biomedicines10071510.
[101] D. Ezhilarasan, V.S. Apoorva, N. Ashok Vardhan, Syzygium cumini extract induced reactive oxygen species-mediated apoptosis in human oral squamous carcinoma cells, J. Oral Pathol. Med. 48 (2019) 115–121, https://doi.org/10.1111/jop.12806.
[102] J. Cao, M.B. Zhong, C.A. Toro, L. Zhang, D. Cai, Endo-lysosomal pathway and ubiquitin-proteasome system dysfunction in Alzheimer's disease pathogenesis, Neurosci. Lett. 703 (2019) 68–78, https://doi.org/10.1016/j.neulet.2019.03.016.
[103] T. Nuzzo, M. Feligioni, L. Cristino, I. Pagano, S. Marcelli, F. Iannuzzi, R. Imperatore, L. D'Angelo, C. Petrella, M. Carella, L. Pollegioni, S. Sacchi, D. Punzo, P. De Girolamo, F. Errico, N. Canu, A. Usiello, Free D-aspartate triggers NMDA receptor-dependent cell death in primary cortical neurons and perturbs JNK activation, Tau phosphorylation, and protein SUMOylation in the cerebral cortex of mice lacking D-aspartate oxidase activity, Exp. Neurol. 317 (2019) 51–65, https://doi.org/10.1016/j.expneurol.2019.02.014.
[104] A. Theerasri, S. Janpaijit, T. Tencomnao, A. Prasansuklab, Beyond the classical amyloid hypothesis in Alzheimer's disease: molecular insights into current concepts of pathogenesis, therapeutic targets, and study models, WIREs Mechanisms of Disease 15 (2023), https://doi.org/10.1002/wsbm.1591.
[105] D. Puzzo, L. Lee, A. Palmeri, G. Calabrese, O. Arancio, Behavioral assays with mouse models of Alzheimer's disease: practical considerations and guidelines, Biochem. Pharmacol. 88 (2014) 450–467, https://doi.org/10.1016/j.bcp.2014.01.011.
[106] D.-J. Hwang, H.-S. Um, D.-H. Choi, J.-Y. Cho, Neuroprotective effects of high-intensity interval training through neuroplastic changes in a restraint stress-induced depression model, Appl. Sci. 13 (2023) 7680, https://doi.org/10.3390/app13137680.